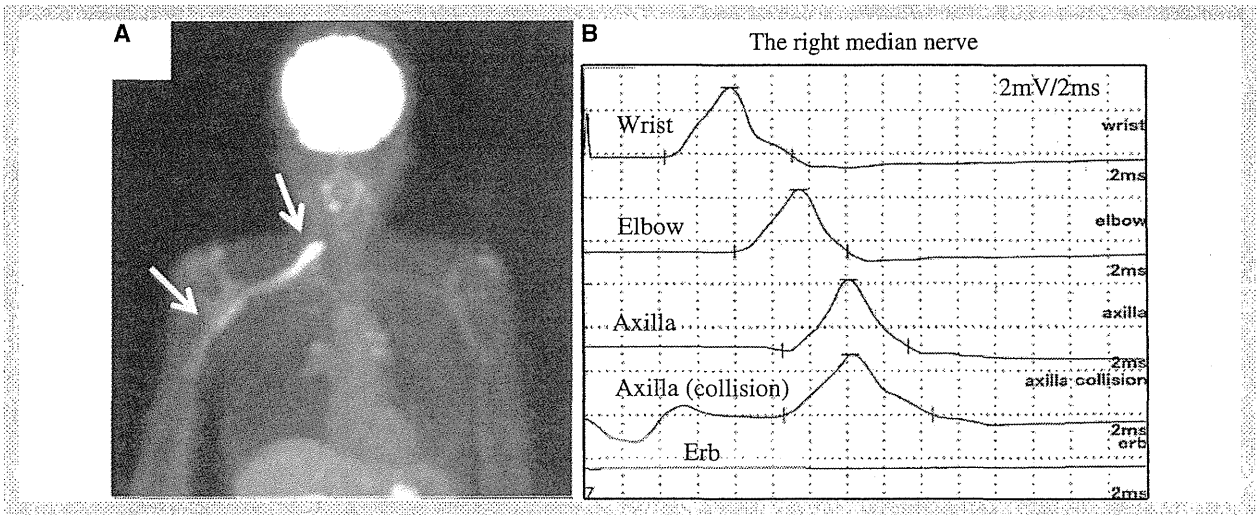


**Figure 2** Findings of whole-body FDG-PET and nerve conduction studies in Patient 10, who had diffuse large B cell lymphoma. (**A**) Accumulation of FDG along the right brachial plexus (arrow) was observed. (**B**) A conduction block was present between the erb and the axilla, which was located between the proximal and distal portion of the nerve segments, with increasing FDG uptake.

## Features of neurolymphomatosis

### Pathologically-proven neurolymphomatosis

Nine patients (Patients 1–9) were pathologically confirmed as having neurolymphomatosis. The lymphoma in this group was primarily of the B cell type, as only two patients (Patients 5 and 7) exhibited the T cell type (Table 1). The most common type was diffuse large B cell lymphoma, which was present in six of nine patients. The mode of progression was subacute to chronic in these patients. The neuropathic features included local peripheral nerve involvement, such as multiple mononeuropathy in the extremities or cranial nerves in seven patients (Patients 1–7). The other two patients (Patients 8 and 9) manifested symmetrical polyneuropathy (Fig. 1 and Table 2). Spontaneous pain in the affected extremities was reported in six of nine patients. Three of these patients (Patients 1, 2 and 6) complained of severe pain that disrupted routine activities.

Nerve conduction studies revealed some degree of reduced compound muscle and sensory nerve action potentials in all of these patients (Supplementary Table 3), and demyelinating features were also concomitantly observed in some patients. Three of these patients (Patients 4, 8 and 9) met the EFNS/PNS electrodiagnostic criteria of definite CIDP (Joint Task Force of the EFNS and the PNS, 2010) (Table 2).

Sural nerve biopsy specimens were obtained from seven of these patients (Patients 1, 3, 4, 5, 7, 8 and 9) (Supplementary Table 1). These specimens showed a reduction of myelinated fibres to varying extents. A mild to moderate reduction of the unmyelinated fibre density was also observed in these specimens. Teased-fibre preparations revealed axonal degeneration with only minor demyelinating changes. Lymphomatous cell invasion was observed in five of these patients (Patients 3, 4, 5, 7 and 9). The regions of lymphomatous cell invasion were primarily observed in and around the perineurium, particularly the subperineurium, with extension into the inner space of the endoneurium. Epineurial lymphomatous cell invasion was also observed in one patient (Patient 9). In Patient 6, a biopsy of the tumour in the left sciatic nerve was performed, and the patient was diagnosed with lymphoma.

Autopsied specimens were obtained from four patients (Supplementary Table 2). An invasion of lymphomatous cells was observed in all of these patients (Figs 3 and 4) and was conspicuous in the proximal portions of the PNS, such as the nerve roots and proximal portions of the nerve trunks. The mode of lymphomatous cell invasion into the nerve was similar to that in the sural nerve biopsy specimens, as cell infiltration was prominent in and around the perineurium, particularly the subperineurium, with extension into the inner space of the endoneurium. Lymphomatous cells were observed along the pia mater of the spinal cord (Patient 1), but no invasion of these cells into the parenchyma was observed. The invasion of lymphomatous cells was not observed in the dorsal root ganglia, thoracic sympathetic ganglia, or spinal cord (Patients 2, 7 and 8).

Invading lymphomatous cells in the PNS of this group showed an obvious atypical cellular appearance (Fig. 3B), leading to a diagnosis of neurolymphomatosis. The diagnoses were also supported by evidence from additional immunohistochemical studies for each specific diagnosis of lymphoma (Supplementary Table 4). *In situ* hybridization of small ribonucleic acids of Epstein-Barr virus was performed in five of six cases with diffuse large B cell lymphoma (Asano *et al.*, 2009), and the results were negative (Supplementary Table 4).

Demyelination was observed at sites of lymphomatous cell invasion (Fig. 4). Nerves with demyelination were not in direct contact with lymphomatous cells. The direct attachment of lymphomatous cells to the Schwann cells of myelinated and

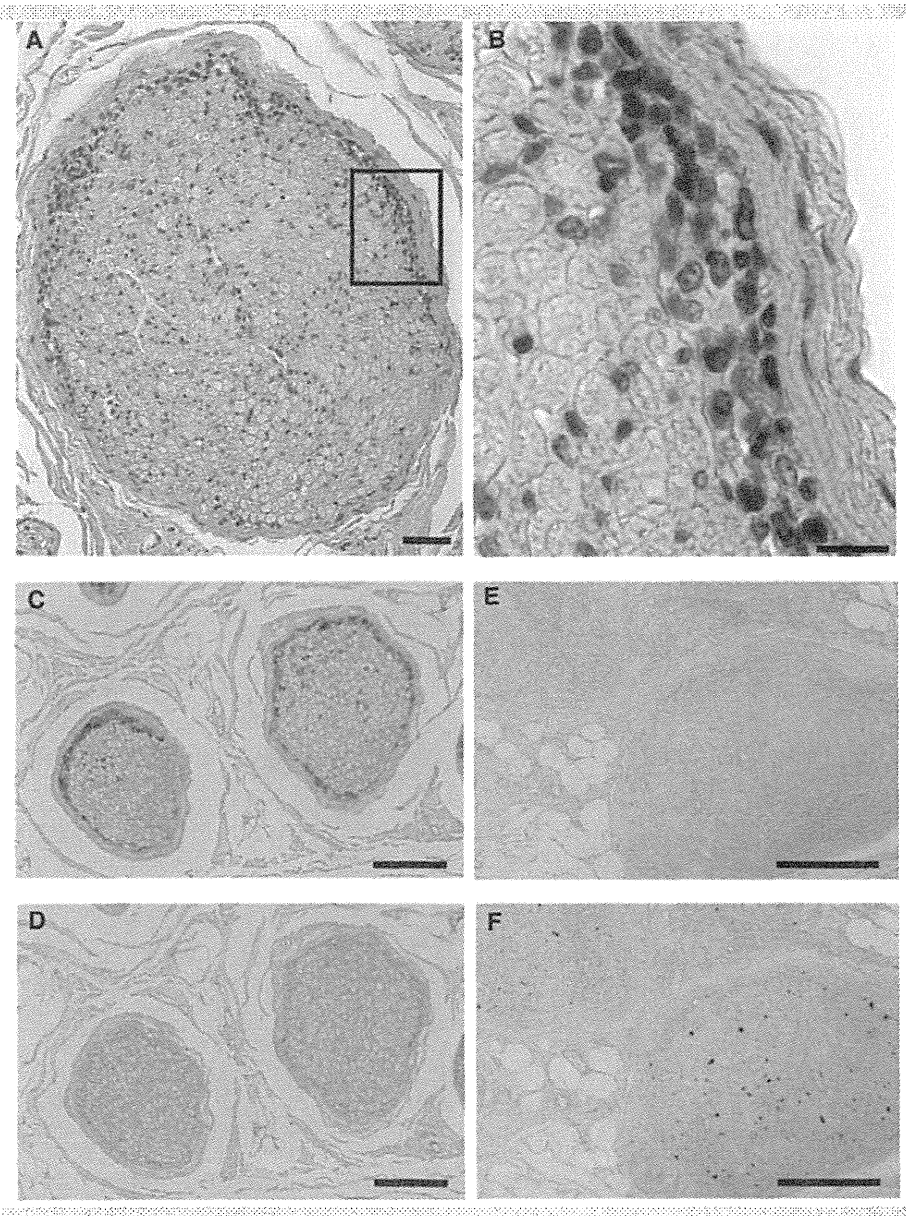


**Figure 3** Sciatic nerve from Patient 1 with diffuse large B cell lymphoma. (**A**) Invasion of lymphomatous cells was primarily observed in the subperineurium through haematoxylin-eosin staining. Cross section. (**B**) In a high power view, invading cells exhibited atypical cellular appearance. (**C**) Lymphomatous cell invasion was observed in the proximal portion of the sciatic nerve after immunostaining with CD20 as a marker of B cell lymphoma. (**D**) Macrophages were not observed after immunostaining with CD68 in the proximal portion of the sciatic nerve with lymphomatous cell invasion. (**E**) Lymphomatous cell invasion was not observed after immunostaining with CD20 in the distal portion of the sciatic nerve with axonal degeneration. (**F**) Macrophages were abundantly observed after immunostaining with CD68 in the distal portion of the sciatic nerve, where axonal degeneration was observed. Scale bars: **A** = 50 μm; **B** = 20 μm; **C–F** = 200 μm.

unmyelinated fibres was not observed. Macrophages were not observed at demyelinating sites (Figs 3C–F and 4). In contrast, axonal degeneration was conspicuous in the distal portions of the nerve trunk. Axonal degeneration was observed without lymphomatous cell invasion in the nerve trunk distal from the sites of the lymphomatous cell invasion and demyelination. Rather, macrophages were abundantly present in the regions of the nerves where the axonal degeneration was conspicuous (Fig. 3F). These findings suggest that demyelination in lesions with lymphomatous cell invasion is not associated with macrophage infiltration but, rather, induces axonal degeneration with the infiltration of macrophages in the distal portion. These findings were similar in all four autopsied cases examined. A representative case is described in the Supplementary material.

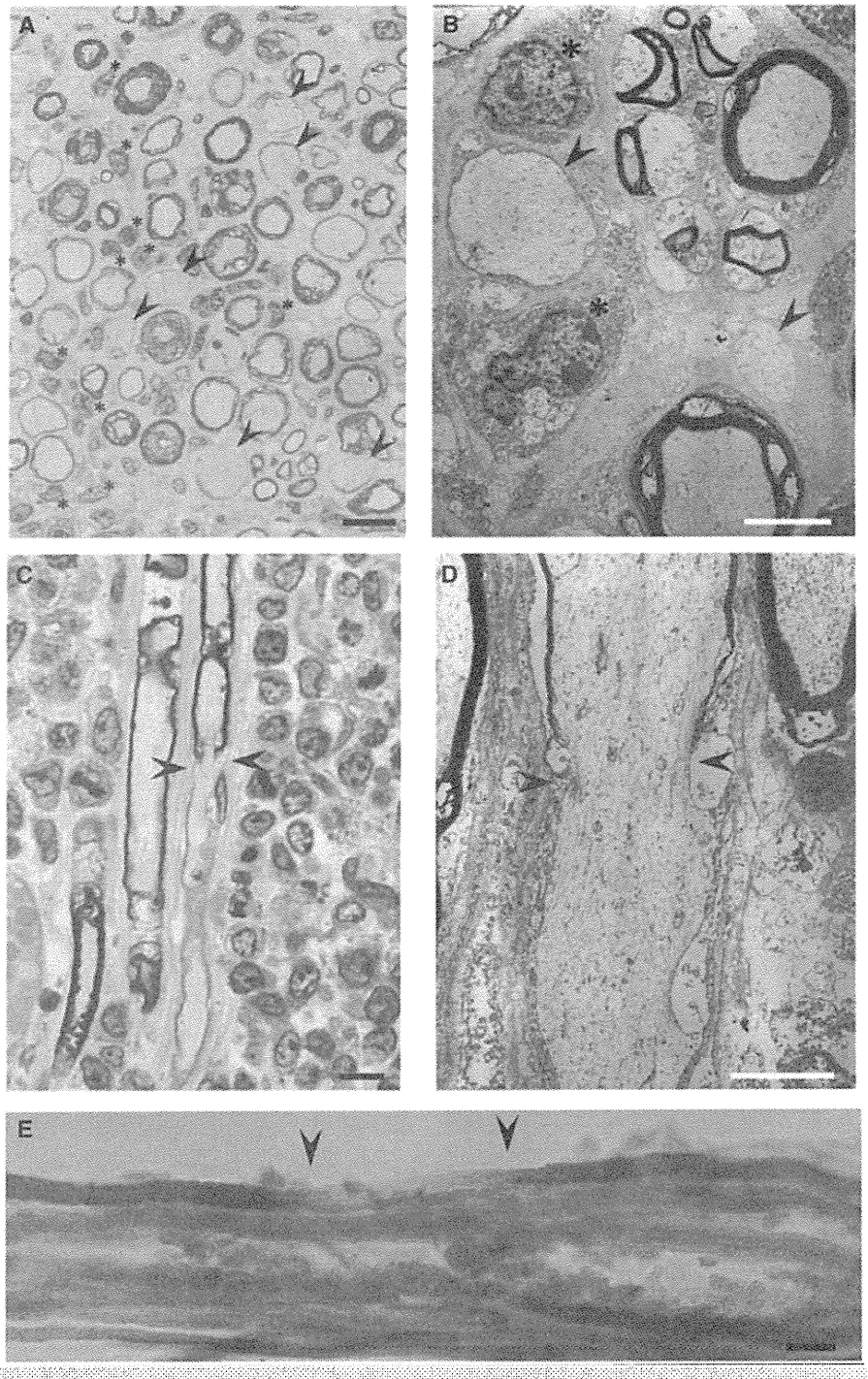


**Figure 4** L4 anterior root from Patient 8 with Burkitt's lymphoma. (**A**) Demyelination (arrowhead) was observed near the infiltration of lymphomatous cells (asterisk) in toluidine blue-stained semi-thin cross sections. (**B**) Demyelination (arrowhead) near the infiltration of lymphomatous cells (asterisk) was confirmed through electron microscopy. Uranyl acetate and lead citrate stain. (**C**) The myelin sheath disappeared at the arrowhead in semi-thin longitudinal sections. Toluidine blue stain. Mononuclear cells with an atypical cellular appearance were abundant around the site of demyelination. (**D**) The disappearance of the myelin sheath was confirmed through electron microscopy (arrowhead). Uranyl acetate and lead citrate stain. (**E**) Demyelination was also observed at the site of lymphomatous cell infiltration in the teased-fibre study (arrowhead). Scale bars: **A** and **C** = 10 μm; **B** and **D** = 5 μm; **E** = 20 μm.

### Neurolymphomatosis assessed through fluorodeoxyglucose positron emission tomography

All six patients (Patients 10–15) who exhibited an accumulation of FDG along the peripheral nerves on FDG-PET imaging had B cell lymphoma, and five patients had diffuse large B cell lymphoma (Table 1). The accumulation of FDG was observed at the brachial plexus in four patients (Patients 10, 11, 14 and 15) and at the lumbar plexus in two patients (Patients 12 and 13) (Table 1, Fig. 2A and Supplementary Fig. 2). In Patient 10, a conduction block was present between the erb and the axilla (Fig. 2B), located between the proximal and distal portions of nerve segments with increasing FDG uptake. This finding indicates that lymphoma cell invasion was present in the brachial plexus and that segmental demyelination was present at this lesion.

Neuropathic features were characterized according to the locality of the peripheral nerve involvement represented as multiple mononeuropathy in the extremities in all patients (Fig. 1 and Table 2). Three patients also manifested unilateral cranial nerve involvement. The mode of progression was subacute to chronic. Spontaneous pain in the affected extremities was reported in all patients. Nerve conduction studies revealed some degree of axonal features in all patients, but demyelinating features were also conspicuously observed in two of these patients (Patients 10 and 15), fulfilling the EFNS/PNS electrodiagnostic criteria of definite CIDP (Joint Task Force of the EFNS and the PNS, 2010) (Supplementary Table 3). The clinical and electrophysiological features were similar to those of pathologically-proven neurolymphomatosis. A representative case is described in the Supplementary material.

## Features of paraneoplastic neuropathy

### CIDP-type neuropathy

Three patients (Patients 16–18) categorized as 'paraneoplastic CIDP-type' showed subacute to chronic sensorimotor polyneuropathy with a symmetrical manifestation (Fig. 1 and Table 2). In contrast to the patients suspected as having neurolymphomatosis, none of these patients had diffuse large B cell lymphoma, and two of the three patients had T cell lymphoma (Table 1). The electrophysiological features revealed a marked prolongation of the distal latency and a reduction of the conduction velocity (Supplementary Table 3). Two patients (Patients 17 and 18) fulfilled the EFNS/PNS electrodiagnostic criteria of definite CIDP (Joint Task Force of the EFNS and the PNS, 2010). In addition, a reduction of compound muscle action potential was observed in these patients. The sural nerve biopsy findings of these patients revealed extensive segmental demyelination in the teased-fibre preparations (21, 31 and 34% for Patients 16, 17 and 18, respectively) without lymphomatous cell invasion (Supplementary Table 1). Axonal degeneration with a reduction of the myelinated fibre density was also conspicuous in Patients 16 and 17 (58 and 43%, respectively). However, the reduction of unmyelinated fibres was not conspicuous relative to the loss of myelinated fibres. FDG-PET was performed in Patient 17, and no invasion into the PNS was observed. A representative case is described in the Supplementary material.

### Sensory ganglionopathy

A patient (Patient 19) with diffuse large B cell lymphoma manifested sensory ataxia in the extremities arising from proprioceptive and kinaesthetic sensory loss. The electrophysiological features revealed a reduction of sensory nerve action potentials (Supplementary Table 3). The sural nerve biopsy findings revealed a predominant large-fibre loss (Supplementary Table 1). In addition, motor nerve conduction studies revealed findings suggestive of demyelination, consistent with previous reports (Camdessanché *et al.*, 2002). The autopsy revealed a loss of neurons in the dorsal root ganglia with the preservation of motor neurons in the spinal cord and an absence of lymphomatous cell invasion into the PNS (Supplementary Table 2).

### Vasculitic neuropathy

A patient (Patient 20) with diffuse large B cell lymphoma, categorized as having 'paraneoplastic vasculitic neuropathy', showed subacute symmetrical sensorimotor polyneuropathy (Fig. 1 and Table 2). The electrophysiological features suggested predominant axonal neuropathy (Supplementary Table 3). The sural nerve biopsy findings revealed an occlusion of small vessels in the epineurium with inflammatory cellular infiltration without an atypical cellular appearance (Supplementary Table 1).

## Features of unclassified group

### Multiple mononeuropathy

All 10 patients (Patients 21–30) in this group had B cell lymphoma, and seven patients had diffuse large B cell lymphoma (Table 1). Neuropathic features were characterized by the locality of the peripheral nerve involvement, as represented by multiple mononeuropathy in the extremities or unilateral cranial nerve involvement (Table 2 and Supplementary Fig. 1). Spontaneous pain in the affected extremities was reported in five patients. Patient 21 complained of severe pain significantly disrupting daily activities, which is similar to the pain experienced by patients with neurolymphomatosis. In addition, the cytology of the CSF was positive in Patient 28. Nerve conduction studies revealed some degree of reduction of compound muscle action potentials and sensory nerve action potentials in all of these patients (Supplementary Table 3), and demyelinating features were also concomitantly observed in some patients. Three patients (Patients 22, 24 and 25) fulfilled the EFNS/PNS electrodiagnostic criteria of definite CIDP (Joint Task Force of the EFNS and the PNS, 2010). Clinical and electrophysiological features of patients in this group were more similar to those of neurolymphomatosis than those of paraneoplastic neuropathy, except for Patient 30, who manifested acutely progressive sensorimotor neuropathy compatible with the definition of Guillain-Barré syndrome (Asbury and Cornblath, 1990).

Sural nerve biopsy specimens were obtained from seven of 10 patients (Supplementary Table 1). These specimens revealed a reduction of myelinated fibres to varying extents. A moderate to severe reduction of unmyelinated fibre density was also observed. Teased-fibre preparations revealed axonal degeneration with few demyelinating changes. Lymphomatous cell invasion was not

observed in these cases. In Patient 25, several fibres with segmental demyelination at consecutive nodes of Ranvier were observed. Considering the concomitant observation of axonal degeneration, demyelination in these fibres was considered secondary to axonal atrophy rather than primary demyelination (Dyck *et al.*, 1981). A representative case is described in the Supplementary material.

### Polyneuropathy

These patients (Patients 31 and 32) had T cell lymphoma (Table 1). Both patients showed a symmetrical polyneuropathy pattern, and their electrophysiological features were characterized by axonal involvement (Table 2, Supplementary Fig. 1 and Supplementary Table 3). The mode of neuropathy progression was acute in both patients, and Patient 31 became unable to walk within 1 month, mimicking the course of Guillain-Barré syndrome. Paraneoplastic aetiology was suspected in this patient, whereas the invasion of lymphomatous cells may have been present in Patient 32, as the cytology of the CSF was positive.

## Treatments and outcomes

The details of treatments and outcomes are listed in Table 3. Immunomodulatory treatment was administered in nine of 15 patients (Patients 1–3, 5, 7, 9 and 13–15) diagnosed as having neurolymphomatosis. As the diagnosis of lymphoma was delayed in seven patients (Patients 1, 3, 5, 7 and 13–15), immunomodulatory treatment for neuropathy was performed before antineoplastic therapies were administrated. In Patients 2 and 9, immunomodulatory treatments were performed after chemotherapy. Intravenous immunoglobulin (IVIg; 400 mg/kg/day for 5 days) and high-dose intravenous methylprednisolone (1000 mg/day for 3 days) were administered alone or in combination. One of seven patients responded to the IVIg therapy, whereas six of the seven patients responded to some degree to the intravenous methylprednisolone. Plasma exchange was performed in Patient 7, which was slightly effective. However, the effects of these treatments were only partial and transient; therefore, repetitive treatments were needed, and most patients eventually deteriorated despite the multiple treatments.

Among patients diagnosed as having paraneoplastic neuropathy, two of the three patients, with features of CIDP (Patients 17 and 18), were administered an immunomodulatory treatment, and these patients responded well. One patient (Patient 17) was treated with IVIg, and the other (Patient 18) was treated with intravenous methylprednisolone. A patient with sensory ganglionopathy (Patient 19) also responded temporarily to immunomodulatory treatments.

For the 10 patients categorized as having 'unclassified multiple mononeuropathy', IVIg or intravenous methylprednisolone was administered alone or in combination. Two of five patients treated with IVIg therapy responded to the treatment, and two of five patients treated with intravenous methylprednisolone therapy responded to the treatment. Among the patients categorized as having 'unclassified polyneuropathy', the response to immunomodulatory treatment was favourable in Patient 31, although the recurrence of similar episodes was frequent (four times within 25 months).

Overall, the response to the immunomodulatory treatments was better in patients with paraneoplastic neuropathy than in those with neurolymphomatosis. The response of the patients with 'unclassified multiple mononeuropathy' appeared to be similar to that of patients with neurolymphomatosis rather than those with paraneoplastic neuropathy.

The effect of chemotherapy on neuropathy was assessed in 21 patients. In 13 of the 21 patients treated with chemotherapy, the neurological deficits improved after the chemotherapy for lymphoma. The effect was positive in eight of the 14 patients with neurolymphomatosis, in one of the two patients with 'paraneoplastic CIDP-type', and in two of the three patients with 'unclassified multifocal mononeuropathy'. Intrathecal chemotherapy was administered in eight patients (Patients 2, 5, 8, 11 to 13, 24 and 32). The 5-year overall survival rate was 48%. In the patients with diffuse large B cell lymphoma, the 5-year overall survival rate was 39%.

Spontaneous pain was reported particularly in patients diagnosed as having neurolymphomatosis. Six patients (Patients 1, 2, 6, 13, 15 and 21) complained of severe pain that significantly disrupted daily activities. Symptomatic therapies for pain included the oral administration of antiepileptic drugs or tricyclic antidepressants, such as carbamazepine, clonazepam, gabapentin, or imipramine, which showed only partial effects. Sacral root block and epidural block were performed in Patients 1 and 21, respectively. Opiates were used in four patients (Patients 2, 6, 13 and 15).

# Discussion

The pathogenesis of neuropathy in the patients with lymphoma is considered diverse. Neuropathies associated with lymphoma are broadly divided into neurolymphomatosis and paraneoplastic neuropathies (Vital *et al.*, 1990; Vallat *et al.*, 1995; Viala *et al.*, 2008; Grisariu *et al.*, 2010; Briani *et al.*, 2011; Baehring and Batchelor, 2012). Thus far, in patients showing multiple mononeuropathies, distal axonopathy arising from the direct invasion of lymphoma cells into the nerve trunk or vasculitis associated with paraneoplastic syndrome has been postulated to cause neuropathy, whereas demyelinating changes arising from humoral factors have been suspected as the major cause of neuropathy in patients showing a symmetric polyneuropathy pattern (Viala *et al.*, 2008). However, the electrophysiological study presented here indicated a more complex mixture of demyelinating and axonal changes in both the multiple mononeuropathy and symmetric polyneuropathy patterns.

In our study, cases with multiple mononeuropathy were more frequent than those with symmetrical polyneuropathy, constituting 23 of 32 (72%) cases. In these cases, 13 patients (57%) were diagnosed as having neurolymphomatosis. Among the other 10 patients manifesting multiple mononeuropathy, the similarities of the clinical and electrophysiological features to those diagnosed as neurolymphomatosis might suggest that the mechanisms underlying neurolymphomatosis cases play a major role in these patients, although we cannot completely rule out the possibility of the participation of paraneoplastic mechanisms in these patients. Patients with pathologically-proven neurolymphomatosis were also included in

Table 3 Treatments and outcomes

| Patients | Effect of immunotherapy on neuropathy | | | Therapy for lymphoma | | Effect of chemotherapy on neuropathy | mRS | | | Follow up duration (months) |
|---|---|---|---|---|---|---|---|---|---|---|
| | IVIg | Steroid | PE | Before neuropathy | After neuropathy | | At admission | Afer treatment | Long-term outcome | |
| Neurolymphomatosis* | | | | | | | | | | |
| 1 | ND | 1+ | ND | | CHOP | 1+ | 3 | 3 | Dead | 14 |
| 2 | – | 1+ | ND | CHOP | Rituximab CHOP MTX** CHASE | – | 3 | 3 | Dead | 7 |
| 3 | 2+ | 2+ | ND | | R-CHOP CODOX-M MTX | 2+ | 5 | 4 | 4 | 75 |
| 4 | ND | ND | ND | MTX R-CHOP | MTX AraC PSL Radiation | 2+ | 3 | 2 | Dead | 65 |
| 5 | – | ND | ND | | AraC** MTX** PSL** | ND | 4 | 4 | Dead | 30 |
| 6 | ND | ND | ND | | CHOP R-DeVIC THP-COP | 2+ | 3 | 1 | 1 | 108 |
| 7 | – | 1+ | 1+ | | VP16 | 2+ | 4 | 3 | Dead | 91 |
| 8 | ND | ND | ND | CVAD | MTX** AraC** Rituximab CPM Dexamethasone** | – | 3 | 3 | Dead | 7 |
| 9 | – | ND | ND | R-CHOP | IMVP-16/CBDCA CHASER | – | 4 | 4 | Dead | 36 |
| 10 | ND | ND | ND | R-CHOP | Rituximab DeVIC | 2+ | 3 | 2 | 2 | 84 |
| 11 | ND | ND | ND | R-CHOP | R-DeVIC MTX** PSL** | 2+ | 3 | 2 | 1 | 69 |
| 12 | ND | ND | ND | EPOCH rituximab | MTX* | – | 4 | 4 | Dead | 12 |
| 13 | ND | 2+ | ND | | MTX** AraC** Dexamethasone** Radiation | – | 3 | 2 | Dead | 9 |
| 14 | – | 2+ | ND | | R-CHOP | 2+ | 3 | 2 | 2 | 29 |
| 15 | – | – | ND | | R-CHP CHASER MTX DeVIC | – | 3 | 4 | Dead | 33 |
| Paraneoplastic neuropathy | | | | | | | | | | |
| CIDP type | | | | | | | | | | |
| 16 | ND | ND | ND | CHOP VP16 MST16 PCZ | MST16 VP16 PSL L-PAM | – | 4 | 5 | Dead | 80 |
| 17 | 2+ | ND | ND | | Rituximab CPM PSL | 2+ | 4 | 3 | 3 | 46 |
| 18 | ND | 2+ | ND | INFγ PUVA Vorinostat | | ND | 4 | 3 | Dead | 132 |
| Sensory ganglionopathy | | | | | | | | | | |
| 19 | 2+ | 2+ | 2+ | | | ND | 5 | 3 | Dead | 92 |

(continued)

Table 3 Continued

| Patients | Effect of immunotherapy on neuropathy | | | Therapy for lymphoma | | Effect of chemotherapy on neuropathy | mRS | | | Follow up duration (months) |
|---|---|---|---|---|---|---|---|---|---|---|
| | IVIg | Steroid | PE | Before neuropathy | After neuropathy | | At admission | Afer treatment | Long-term outcome | |
| Vasculitic neuropathy | | | | | | | | | | |
| 20 | ND | ND | ND | CHOP | | ND | 4 | ND | ND | 24 |
| Unclassified | | | | | | | | | | |
| Multiple mononeuropathy | | | | | | | | | | |
| 21 | 1+ | 1+ | ND | | CODOX-M/IVAC R-CHOP CHASER PBSCT | – | 2 | 2 | Dead | 39 |
| 22 | 2+ | ND | ND | | | ND | 5 | 4 | Dead | 11 |
| 23 | – | ND | ND | | | ND | 3 | 4 | Dead | 3 |
| 24 | ND | 1+ | ND | | MTX** AraC** Dexamethasone** R-CHOP | 1+ | 3 | 3 | Dead | 41 |
| 25 | – | – | ND | Rituximab THP-COP | Rituximab | ND | 4 | 4 | 4 | 68 |
| 26 | ND | ND | ND | R-CHOP F-ara-A MIT | | ND | 4 | ND | ND | 58 |
| 27 | ND | – | ND | CHOP | | ND | 4 | 4 | 5 | 70 |
| 28 | ND | ND | ND | | | ND | 3 | 5 | Dead | 7 |
| 29 | – | – | ND | | | ND | 4 | 5 | Dead | 5 |
| 30 | ND | ND | ND | | CHOP | 1+ | ND | ND | ND | 2 |
| Polyneuropathy | | | | | | | | | | |
| 31 | 2+ | 2+ | ND | | MTX PCZ VCR AraC CHOP PBSCT | 2+ | 3 | 2 | 2 | 129 |
| 32 | 1+ | 1+ | ND | | MTX** AraC** PSL** R-CHOP BMT | 2+ | 2 | 1 | 1 | 120 |

AraC = Cytarabine; BMT = bone marrow transplantation; CDOX-M = Cyclophosphamide, Vincristine, Doxorubicin, Methotrexate; CDOX-M/IVAC = CDOX-M + Etoposide, Ifosfamide, Cytarabine; CHASE = Cyclophosphamide, Cytarabine, Etoposide, Dexamethasone; CHASER = CHASE + Rituximab; CHOP = Cyclophosphamide, Doxorubicin, Vincristine, Prednisolone; CPM = Cyclophosphamide; CVAD = Cyclophosphamide, Vincristine, Doxorubicin, Dexamethasone; DeVIC = Dexamethasone, Etoposide, Ifosfamide, Carboplatin; EPOCH = Etoposide, Prednisolone, Vincristine, Cyclophosphamide, Doxorubicin; F-ara-A = Fludarabine; INF$\gamma$ = Interferon $\gamma$; IMVP-16/CBDCA = Ifosfamide, Methotrexate, Etoposide, Carboplatin; L-PAM = Melphalan; PE = plasma exchange; MIT = Mitoxantrone; MST16 = Perazolin; MTX = Methotrexate; ND = not done; PBSCT = peripheral blood stem cell transplantation; PCZ = Procarbazine; PUVA = psoralen + ultraviolet A; PSL = Prednisolone; R-CHOP = Rituximab + CHOP; R-CHP = Rituximab, Cyclophosphamide, Doxorubicin, Prednisolone; R-DeVIC = Rituximab + DeVIC; THP-COP = Pirarubicin, Cyclophosphamide, Vincristine, Prednisolone; VCR = Vincristine; VP16 = Etoposide.

1+ and 2+ represent slight and good response to treatment, respectively.

*Patients 1 to 9 were pathologically-proven neurolymphomatosis, whereas Patients 10 to 15 were FDG-PET assessed neurolymphomatosis.

**Therapy was done intrathecally.

two of the nine cases manifesting symmetrical polyneuropathy. Therefore, patients who showed asymmetrical features in the early phase might develop the symmetrical polyneuropathy type as the disease advances. In this context, neurolymphomatosis might play a more important role in neuropathy associated with lymphoma than previously suggested. Sural nerve biopsy is limited for the diagnosis of neuropathy associated with lymphoma, as biopsy assesses only a distal portion of the PNS (van den Bent *et al.*, 1999). Notably, only one patient with sensory ganglionopathy, which is the most common form of paraneoplastic neuropathy (Oki *et al.*, 2007; Koike *et al.*, 2011*a*), was included among five patients with pathologically-proven paraneoplastic neuropathy. However, because this is a retrospective study and only patients who were referred to the neurological department of our institute were included, there was a sample bias.

The characteristic findings that explain the cause of neuropathy in most patients included lymphoma cell invasion-associated demyelination and axonal degeneration of the distal portion of the nerve trunk. The invasion of lymphomatous cells into the nerve trunk has been designated as neurolymphomatosis and is reported as a characteristic feature of neuropathy associated with lymphoma (Guberman *et al.*, 1978). In our cases, lymphomatous cells invaded in and around the perineurium, particularly the subperineurium. Because the lymphatic flow is preferentially present in the subperineurial space, this area has an affinity for lymphomatous cells. In addition, the lymphomatous cell invasion continued into the endoneurium. Demyelination was observed at the site of lymphoma cell invasion, and axonal degeneration occurred distal from the site of lymphoma cell invasion. Therefore, demyelination at the site of neurolymphomatosis might be the primary lesion, with axonal degeneration occurring secondarily in most patients with lymphoma-associated neuropathy. This view is supported through electrophysiological findings showing a mixture of demyelinating and axonal changes and sural nerve biopsy findings showing predominant axonal degeneration in the distal portion of the nerves. The demyelination observed in the present study was different from that in acute inflammatory demyelinating polyneuropathy or CIDP, as macrophage-mediated demyelination was not observed in our patients (Prineas and McLeod, 1976). Because lymphomatous cells do not directly contact myelinated fibres or Schwann cells, humoral factors produced by the lymphoma cells close to the myelinated fibres likely play an important role. Future studies are needed to identify the humoral factors that mediate this demyelination. In addition to the reduction of the myelinated fibres, a reduction of unmyelinated fibres was observed. Therefore, primary axonal changes might also occur, to some extent, even in patients with neurolymphomatosis. Considering the fairly well-preserved nerve fibres at the site of demyelination, most axonal changes might secondarily occur distally from the site of the lymphomatous cell invasion. Interestingly, proximal demyelination with distal axonal changes, which is considered as the most common pathogenesis of neuropathy associated with lymphoma, was observed in both B cell and T cell types of lymphoma, although most of the patients had B cell lymphoma. It is also interesting that even patients with diffuse large B cell lymphoma, which was the most common type of lymphoma in the present study, showed a diverse neuropathic presentation, including neurolymphomatosis as well as paraneoplastic demyelination and vasculitis.

The difficulty of the diagnosis of lymphoma-associated neuropathy deserves attention. Neuropathy can occur at any stage of lymphoma, and neuropathic symptoms preceded the detection of lymphoma in approximately half of our patients. Therefore, elucidating the characteristics of neuropathy associated with lymphoma is important because it will enable the early detection of lymphoma and the immediate initiation of therapy for both the lymphoma and the neuropathy itself. The diagnostic pitfalls elucidated in this study include the scarcity of laboratory evidence suggestive of the presence of lymphoma, demyelinating features in the electrophysiological study, and the possible response to immunomodulatory therapies. These features resulted in the physicians recalling the diagnosis of Guillain-Barré syndrome or CIDP in some of the patients, as described in the case presentation (Supplementary material). Indeed, 11 patients in the present study fulfilled the EFNS/PNS electrodiagnostic criteria of definite CIDP (Joint Task Force of the EFNS and the PNS, 2010). However, patients with neurolymphomatosis in our study were characterized by a focality of neuropathic involvement even though the electrophysiological features fulfilled the EFNS/PNS criteria for CIDP, which is considered atypical (Joint Task Force of the EFNS and the PNS, 2010). In addition, the frequent presence of spontaneous pain in our patients would be suggestive of diseases other than CIDP, as pain is not common in CIDP (Nasu *et al.*, 2012). Pain has also been frequently reported in patients with neurolymphomatosis (Grisariu *et al.*, 2010; Baehring and Batchelor, 2012).

Currently, FDG-PET is the most sensitive and specific imaging technique available for patients with lymphoma (Cheson, 2011). In our study, a whole-body FDG-PET was useful for the detection of lymphoma in five of the six patients with lymphoma not observed through conventional means. With respect to patients previously diagnosed as having lymphoma, five of the six patients were positive in the FDG-PET study. Therefore, we should consider that FDG-PET does not necessarily reveal lymphoma in all patients. Case reports suggested the usefulness of this technique in the detection of neurolymphomatosis even in patients with negative MRI, CSF, or bone marrow analysis findings (Salm *et al.*, 2012). However, the specificity of FDG-PET study in the diagnosis of neurolymphomatosis (e.g. differentiation from neurolymphomatosis to CIDP) has not yet been established. In our study, FDG-PET was performed in a patient with paraneoplastic CIDP-type neuropathy (Patient 17). In this patient, no accumulation of FDG was observed in the PNS, although the presence of lymphoma was detected in the iliopsoas muscle.

Serum-soluble interleukin-2 receptor levels offer a rapid, reliable and non-invasive measure of disease activity and response to therapy in a broad spectrum of conditions associated with B or T cell immune activation, including lymphoma (Rubin and Nelson, 1990). Therefore, interleukin-2 receptor is used as an indicator for lymphoma in clinical practice, although it is not specific. Seventeen of the 24 examined patients (71%) showed elevated levels of serum soluble interleukin-2 receptor. Therefore, a high level of serum-soluble interleukin-2 receptor might lead to a suspicion of the concomitance of lymphoma in a patient with

neuropathy, although a normal level does not exclude the possibility of lymphoma.

Immunomodulatory treatment was more or less effective, particularly in the early phase of neuropathy, even in patients with neurolymphomatosis, potentially leading to the misdiagnosis of the cause of neuropathy. Because antineoplastic therapy is essential for the treatment of lymphoma, early diagnosis is necessary for neuropathy associated with lymphoma. The presence of the high degree of axonal loss irrespective of the type of neuropathy might also support this view. However, the response to the immunomodulatory treatments appeared to be better in patients with paraneoplastic neuropathies than in those with neurolymphomatosis; thus, immunomodulatory treatment before, during, or after antineoplastic therapy might also be beneficial for paraneoplastic neuropathy. The outcome determined by the 5-year survival rate in patients with non-Hodgkin's lymphoma with CNS involvement is generally poor, ranging from 14–20% (Hollender *et al.*, 2000; Kridel and Dietrich, 2011). In contrast, the outcome of neuropathy associated with lymphoma was better in our study, although the outcome was poorer than that for lymphoma overall (The Non-Hodgkin's Lymphoma Classification Project, 1997; Feugier *et al.*, 2005).

In conclusion, patients with lymphoma can manifest various neuropathic patterns, and neurolymphomatosis is the major cause of neuropathy. Demyelination unrelated to macrophages at the site of lymphomatous cell invasion and axonal degeneration distal from the site of the lymphomatous cell invasion were the most prominent pathologies of this type of neuropathy. The misdiagnosis of neurolymphomatosis as CIDP is frequent due to the presence of a demyelinating pattern and the initial response to immunomodulatory treatments in patients with neurolymphomatosis. The possibility of the concomitance of lymphoma should be actively considered in various types of neuropathy even if the neuropathy meets the diagnostic criteria of CIDP, particularly in patients complaining of pain.

# Funding

This work was supported by grants from the Ministry of Health, Labour and Welfare (Research on Intractable Diseases, H23-012).

# Supplementary material

Supplementary material is available at *Brain* online.

# References

Antoine JC, Camdessanché JP. Peripheral nervous system involvement in patients with cancer. Lancet Neurol 2007; 6: 75–86.

Asbury AK, Cornblath DR. Assessment of current diagnostic criteria for Guillain-Barré syndrome. Ann Neurol 1990; 27 (Suppl): S21–4.

Asano N, Oshiro A, Matsuo K, Kagami Y, Ishida F, Suzuki R, et al. Prognostic significance of T-cell or cytotoxic molecules phenotype in classical Hodgkin's lymphoma: a clinicopathologic study. J Clin Oncol 2006; 24: 4626–33.

Asano N, Suzuki R, Kagami Y, Ishida F, Kitamura K, Fukutani H, et al. Clinicopathologic and prognostic significance of cytotoxic molecule expression in nodal peripheral T-cell lymphoma, unspecified. Am J Surg Pathol 2005; 29: 1284–93.

Asano N, Yamamoto K, Tamaru J, Oyama T, Ishida F, Ohshima K, et al. Age-related Epstein-Barr virus (EBV)-associated B-cell lymphoproliferative disorders: comparison with EBV-positive classic Hodgkin lymphoma in elderly patients. Blood 2009; 113: 2629–36.

Baehring JM, Batchelor TT. Diagnosis and management of neurolymphomatosis. Cancer J 2012; 18: 463–8.

Baehring JM, Damek D, Martin EC, Betensky RA, Hochberg FH. Neurolymphomatosis. Neuro Oncol 2003; 5: 104–15.

Bosch EP, Habermann TM, Tefferi A. Peripheral neuropathy associated with lymphoma, leukemia, and myeloproliferative disorders. In: Dyck PJ, Thomas PK, editors. Peripheral neuropathy. 4th edn. Philadelphia: Elsevier Saunders; 2005. p. 2489–503.

Briani C, Vitaliani R, Grisold W, Honnorat J, Graus F, Antoine JC, et al. Spectrum of paraneoplastic disease associated with lymphoma. Neurology 2011; 76: 705–10.

Camdessanché JP, Antoine JC, Honnorat J, Vial C, Petiot P, Convers P, et al. Paraneoplastic peripheral neuropathy associated with anti-Hu antibodies. A clinical and electrophysiological study of 20 patients. Brain 2002; 125: 166–75.

Campo E, Swerdlow SH, Harris NL, Pileri S, Stein H, Jaffe ES. The 2008 WHO classification of lymphoid neoplasms and beyond: evolving concepts and practical applications. Blood 2011; 117: 5019–32.

Cheson BD. Role of functional imaging in the management of lymphoma. J Clin Oncol 2011; 29: 1844–54.

Correale J, Monteverde DA, Bueri JA, Reich EG. Peripheral nervous system and spinal cord involvement in lymphoma. Acta Neurol Scand 1991; 83: 45–51.

Dyck PJ, Dyck PJB, Engelstad J. Pathologic alterations of nerves. In: Dyck PJ, Thomas PK, editors. Peripheral neuropathy. 4th edn. Philadelphia: Elsevier Saunders; 2005. p. 733–829.

Dyck PJ, Lais AC, Karnes JL, Sparks M, Hunder H, Low PA, et al. Permanent axotomy, a model of axonal atrophy and secondary segmental demyelination and remyelination. Ann Neurol 1981; 9: 575–83.

Feugier P, van Hoof A, Sebban C, Solal-Celigny P, Bouabdallah R, Fermé C, et al. Long-term results of the R-CHOP study in the treatment of elderly patients with diffuse large B-cell lymphoma: a study by the Groupe d'Etude des Lymphomes de l'Adulte. J Clin Oncol 2005; 23: 4117–26.

Giglio P, Gilbert MR. Neurologic complications of non-Hodgkin's lymphoma. Curr Hematol Malig Rep 2006; 1: 214–9.

Graus F, Delattre JY, Antoine JC, Dalmau J, Giometto B, Grisold W, et al. Recommended diagnostic criteria for paraneoplastic neurological syndromes. J Neurol Neurosurg Psychiatry 2004; 75: 1135–40.

Grisariu S, Avni B, Batchelor TT, van den Bent MJ, Bokstein F, Schiff D, et al. Neurolymphomatosis: an International Primary CNS Lymphoma Collaborative Group report. Blood 2010; 115: 5005–11.

Guberman A, Rosenbaum H, Braciale T, Schlaepfer WW. Human neurolymphomatosis. J Neurol Sci 1978; 36: 1–12.

Harris NL, Jaffe ES, Stein H, Banks PM, Chan JK, Cleary ML, et al. A revised European-American classification of lymphoid neoplasms: a proposal from the International Lymphoma Study Group. Blood 1994; 84: 1361–92.

Hollender A, Kvaloy S, Lote K, Nome O, Holte H. Prognostic factors in 140 adult patients with non-Hodgkin's lymphoma with systemic central nervous system (CNS) involvement. A single centre analysis. Eur J Cancer 2000; 36: 1762–8.

Hughes RA, Britton T, Richards M. Effects of lymphoma on the peripheral nervous system. J R Soc Med 1994; 87: 526–30.

Joint Task Force of the EFNS and the PNSEuropean Federation of Neurological Societies/Peripheral Nerve Society Guideline on management of chronic inflammatory demyelinating polyradiculoneuropathy: report of a joint task force of the European Federation of Neurological Societies and the Peripheral Nerve Society–first revision. J Peripher Nerv Syst 2010; 15: 1–9.

Kelly JJ, Karcher DS. Lymphoma and peripheral neuropathy: a clinical review. Muscle Nerve 2005; 31: 301–13.

Kobayashi M, Kato K, Funakoshi K, Watanabe S, Toyoshima I. Neuropathology of paraneoplastic neuropathy with anti-disialosyl antibody. Muscle Nerve 2005; 32: 216–22.

Kohut H. Unusual involvement of the nervous system in generalized lymphoblastoma. J Nerv Ment Dis 1946; 103: 9–20.

Koike H, Tanaka F, Sobue G. Paraneoplastic neuropathy: wide-ranging clinicopathological manifestations. Curr Opin Neurol 2011a; 24: 504–10.

Koike H, Atsuta N, Adachi H, Iijima M, Katsuno M, Yasuda T, et al. Clinicopathological features of acute autonomic and sensory neuropathy. Brain 2010; 133: 2881–96.

Koike H, Hirayama M, Yamamoto M, Ito H, Hattori N, Umehara F, et al. Age associated axonal features in HNPP with 17p11.2 deletion in Japan. J Neurol Neurosurg Psychiatry 2005; 76: 1109–14.

Koike H, Iijima M, Mori K, Yamamoto M, Hattori N, Katsuno M, et al. Nonmyelinating Schwann cell involvement with well-preserved unmyelinated axons in CMT1A. J Neuropathol Exp Neurol 2007; 66: 1027–36.

Koike H, Iijima M, Mori K, Yamamoto M, Hattori N, Watanabe H, et al. Neuropathic pain correlates with myelinated fibre loss and cytokine profile in POEMS syndrome. J Neurol Neurosurg Psychiatry 2008b; 79: 1171–9.

Koike H, Iijima M, Sugiura M, Mori K, Hattori N, Ito H, et al. Alcoholic neuropathy is clinicopahthologically distinct form thiamine-deficiency neuropathy. Ann Neurol 2003; 54: 19–29.

Koike H, Kawagashira Y, Iijima M, Yamamoto M, Hattori N, Tanaka F, et al. Electrophysiological features of late-onset transthyretin Met30 familial amyloid polyneuropathy unrelated to endemic foci. J Neurol 2008a; 255: 1526–33.

Koike H, Kiuchi T, Iijima M, Ueda M, Ando Y, Morozumi S, et al. Systemic but asymptomatic transthyretin amyloidosis 8 years after domino liver transplantation. J Neurol Neurosurg Psychiatry 2011b; 82: 1287–90.

Koike H, Misu K, Sugiura M, Iijima M, Mori K, Yamamoto M, et al. Pathologic difference of early- vs late-onset TTR Met30 familial amyloid polyneuropathy. Neurology 2004; 63: 129–38.

Koike H, Mori K, Misu K, Hattori N, Ito H, Hirayama M, et al. Painful alcoholic polyneuropathy with predominant small-fiber loss and normal thiamine status. Neurology 2001; 56: 1727–32.

Kridel R, Dietrich PY. Prevention of CNS relapse in diffuse large B-cell lymphoma. Lancet Oncol 2011; 12: 1258–66.

MacKintosh FR, Colby TV, Podolsky WJ, Burke JS, Hoppe RT, Rosenfelt FP, et al. Central nervous system involvement in non-Hodgkin's lymphoma: an analysis of 105 cases. Cancer 1982; 49: 586–95.

Moore RY, Oda Y. Malignant lymphoma with diffuse involvement of the peripheral nervous system. Neurology 1962; 12: 186–92.

Nasu S, Misawa S, Sekiguchi Y, Shibuya K, Kanai K, Fujimaki Y, et al. Different neurological and physiological profiles in POEMS syndrome and chronic inflammatory demyelinating polyneuropathy. J Neurol Neurosurg Psychiatry 2012; 83: 476–9.

Oki Y, Koike H, Iijima M, Mori K, Hattori N, Katsuno M, et al. Ataxic vs painful form of paraneoplastic neuropathy. Neurology 2007; 69: 564–72.

Prineas JW, McLeod JG. Chronic relapsing polyneuropathy. J Neurol Sci 1976; 27: 427–58.

Rubin LA, Nelson DL. The soluble interleukin-2 receptor: biology, function, and clinical application. Ann Intern Med 1990; 113: 619–27.

Salm LP, van der Hiel B, Stokkel MP. Increasing importance of 18F-fluorodeoxyglucose PET in the diagnosis of neurolymphomatosis. Nucl Med Commun 2012; 33: 907–16.

Sobue G, Hashizume Y, Mukai E, Hirayama M, Mitsuma T, Takahashi A. X-linked recessive bulbospinal neuronopathy, a clinicopathological study. Brain 1989; 112: 209–32.

Sobue G, Hashizume Y, Yasuda T, Mukai E, Kumagai T, Mitsuma T, et al. Phosphorylated high molecular weight neurofilament protein in lower motor neurons in amyotrophic lateral sclerosis and other neurodegenerative diseases involving ventral horn cells. Acta Neuropathol 1990b; 79: 402–8.

Sobue G, Nakao N, Murakami K, Yasuda T, Sahashi K, Mitsuma T, et al. Type I familial amyloid polyneuropathy. a pathological study of the peripheral nervous system. Brain 1990a; 113: 903–19.

Suzuki K, Katsuno M, Banno H, Takeuchi Y, Atsuta N, Ito M, et al. CAG repeat size correlates to electrophysiological motor and sensory phenotypes in SBMA. Brain 2008; 131: 229–39.

The Non-Hodgkin's Lymphoma Classification ProjectA clinical evaluation of the International Lymphoma Study Group classification of non-Hodgkin's lymphoma. Blood 1997; 89: 3909–18.

Vallat JM, de Mascarel HA, Bordessoule D, Jauberteau MO, Tabaraud F, Gelot A, et al. Non-Hodgkin malignant lymphomas and peripheral neuropathies-13 cases. Brain 1995; 118: 1233–45.

van den Bent MJ, de Bruin HG, Bos GM, Brutel de la Rivière G, Sillevis Smitt PA. Negative sural nerve biopsy in neurolymphomatosis. J Neurol 1999; 246: 1159–63.

van Swieten JC, Koudstaal PJ, Visser MC, Schouten HJ, van Gijn J. Interobserver agreement for the assessment of handicap in stroke patients. Stroke 1988; 19: 604–7.

Viala K, Béhin A, Maisonobe T, Léger JM, Stojkovic T, Davi F, et al. Neuropathy in lymphoma: a relationship between the pattern of neuropathy, type of lymphoma and prognosis? J Neurol Neurosurg Psychiatry 2008; 79: 778–82.

Vital C, Vital A, Julien J, Rivel J, deMascarel A, Vergier B, et al. Peripheral neuropathies and lymphoma without monoclonal gammopathy: a new classification. J Neurol 1990; 237: 177–85.

Walsh JC. Neuropathy associated with lymphoma. J Neurol Neurosurg Psychiatry 1971; 34: 42–50.

Windebank AJ, Grisold W. Chemotherapy-induced neuropathy. J Peripher Nerv Syst 2008; 13: 27–46.


RESEARCH PAPER

# Spreading of amyotrophic lateral sclerosis lesions—multifocal hits and local propagation?

Teruhiko Sekiguchi,[1] Tadashi Kanouchi,[2] Kazumoto Shibuya,[3] Yu-ichi Noto,[4] Yohsuke Yagi,[5] Akira Inaba,[6] Keisuke Abe,[7] Sonoko Misawa,[3] Satoshi Orimo,[6] Takayoshi Kobayashi,[7] Tomoyuki Kamata,[5] Masanori Nakagawa,[4] Satoshi Kuwabara,[3] Hidehiro Mizusawa,[1] Takanori Yokota[1]

► Additional material is published online only. To view please visit the journal online (http://dx.doi.org/10.1136/jnnp-2013-305617).

For numbered affiliations see end of article.

**Correspondence to**
Dr Takanori Yokota, Department of Neurology and Neurological Science, Graduate School, Tokyo Medical and Dental University, 1-5-45 Yushima Bunkyo-ku, Tokyo 113-8519, Japan; tak-yokota.nuro@tmd.ac.jp

Received 16 April 2013
Revised 27 June 2013
Accepted 17 July 2013
Published Online First 11 September 2013

**To cite:** Sekiguchi T, Kanouchi T, Shibuya K, *et al. J Neurol Neurosurg Psychiatry* 2014;**85**:85–91.

## ABSTRACT

**Objective** To investigate whether or not the lesions in sporadic amyotrophic lateral sclerosis (ALS) originate from a single focal onset site and spread contiguously by prion-like cell-to-cell propagation in the rostrocaudal direction along the spinal cord, as has been hypothesised (the 'single seed and simple propagation' hypothesis).

**Methods** Subjects included 36 patients with sporadic ALS and initial symptoms in the bulbar, respiratory or upper limb regions. Abnormal spontaneous activities in needle electromyography (nEMG)—that is, fibrillation potentials, positive sharp waves (Fib/PSWs) or fasciculation potentials (FPs)—were compared among the unilateral muscles innervated by different spinal segments, especially between the T10 and L5 paraspinal muscles, and between the vastus medialis and biceps femoris. Axon length and the proportion of muscle fibre types, which are both related to motoneuronal vulnerability in ALS, are similar in the paired muscles.

**Results** Fourteen of 36 patients showed a non-contiguous distribution of nEMG abnormalities from the onset site, with skipping of intermediate segments. In eight of them, the non-contiguous pattern was evident between paired muscles with the same motoneuronal vulnerability. The non-contiguously affected lumbosacral lesions involved motoneuron columns horizontally or radially proximate to one another, appearing to form a cluster in four of the eight patients. FPs, known to precede Fib/PSWs, were shown more frequently than Fib/PSWs in all the lumbosacral segments but L5, suggesting that 2nd hits occur at L5 and then spread to other lumbosacral segments.

**Conclusions** In sporadic ALS, the distribution of lower motoneuron involvement cannot be explained by the 'single seed and simple propagation' hypothesis alone. We propose a 'multifocal hits and local propagation' hypothesis instead.

## INTRODUCTION

Amyotrophic lateral sclerosis (ALS) is an incurable progressive neurodegenerative disease in which both the upper (UMN) and lower motoneurons (LMN) are diffusely involved at the end. Recent biological studies have demonstrated the remarkable concept of 'prion-like propagation' of pathogenic proteins, such as tau or α-synuclein, in neurodegenerative diseases.[1 2] According to this hypothesis, the pathogenic proteins are transferred from diseased cells to neighbouring healthy cells; this intercellular transfer then leads to spreading of the lesion. In ALS, in vitro studies have indicated that newly formed aggregates of SOD1, TDP-43 or toxic RNA conformation can act as templates for the subsequent misfolding of the respective native proteins,[3–5] and that aggregated SOD1 can be intercellularly transferred in cultured cells.[6] These suggest that the mechanism of prion-like cell-to-cell propagation also underlies the progression of ALS.

The clinical symptoms of most ALS patients start focally, which had already been confirmed both electrophysiologically[7] and pathologically.[8 9] As we have reviewed in the previous article,[10] recent clinical observations have demonstrated that the clinical symptoms spread contiguously from the onsets into the following broadly divided body regions: the bulbar region, upper limbs, trunk and lower limbs.[11–14] This has prompted us to suppose that ALS lesions simply propagate from a single 'seed' to adjacent cells in a domino-like manner (ie, the 'single seed and simple propagation' hypothesis). Alternatively, it can rest on anatomical proximity with the spreading of ALS lesion from the onset site by diffusion of soluble toxic factors in the extracellular matrix.[15] On the other hand, up to about 30% of sporadic ALS patients have also been found to show non-contiguous spread of symptoms from the bulbar region to the lower limbs or vice versa, skipping the upper limbs and trunk.[14 16] However, compensatory re-innervation by the remaining motoneurons can mask the manifestation of clinical signs until more than one-third of the LMNs for a given muscle are lost.[17] Therefore, whether the lesions actually spread non-contiguously among the spinal segments remains unclear.

Needle electromyography (nEMG) can sensitively detect LMN involvement from each segment separately, even in the presymptomatic stage. For this reason, it is a powerful method for investigating whether or not ALS lesions spread contiguously along the spinal segments. In this study, we used nEMG in the early stage of ALS to demonstrate that LMN involvement cannot be necessarily explained by the 'single seed and simple propagation' hypothesis. We then propose a hypothesis of 'multifocal hits and local propagation.'

## SUBJECTS AND METHODS

### Subjects

We designed this study to investigate whether LMN involvement in sporadic ALS spreads contiguously in the rostrocaudal direction from the onset site. Therefore, of 66 consecutive patients with suspected ALS referred to our hospitals from March 2011 to April 2012, 14 patients with lower limb onset were excluded. One patient with a family history of ALS was also excluded. Forty-two of the remaining 51 patients met the revised El Escorial criteria[18] for clinically definite, clinically probable or clinically probable laboratory-supported ALS, although two patients were excluded because their MRIs indicated lumbar spinal disease, which can influence the results of nEMG. Thus, 40 sporadic ALS patients with bulbar, upper limb, or respiratory symptoms at onset were ultimately included in this study. None of these 40 patients had diabetes or any other complicating neuropathies, which were confirmed by nerve conduction studies (performed on their unilateral median, ulnar, tibial, peroneal and sural nerves).

### Selection of muscles to be examined

Motoneurons with longer axons,[19 20] larger motoneurons[9] and fast-fatigable motoneurons[21] have been described as more vulnerable to damage from ALS. If the pathological process begins at the same time in individual motoneurons with different degrees of vulnerability, then motoneurons that are more vulnerable will degenerate faster than those that are more resistant. Thus the pattern of nEMG abnormalities should be influenced by differences in motoneuronal vulnerability. Therefore, to establish adequate milestones for lesion spreading, we selected two pairs of muscles innervated from different spinal segments but with similar degrees of motoneuronal vulnerability; that is, the length of the innervating motor axons and the ratio of type I muscle fibres differ little between the paired muscles (see online supplementary figure S1). One pair—T10 paraspinalis (T10PS; type I fibre ratio: 62.0% in men, 67.8% in women) and L5 paraspinalis (L5PS; 63.6–65.0%)—was selected from the trunk.[22] The other pair—the deep layer of the vastus medialis (VM) (innervating segment: L3/4; type I fibre ratio: 61.5%) and the long head of the biceps femoris (BF; L5/S1, mainly S1; 66.9%)—was selected from the thigh.[23–27]

If a focal ALS lesion spreads contiguously in the rostrocaudal direction along the spinal segments, nEMG abnormalities in the paired muscles should be found in the muscle innervated by the rostral segment earlier than in the muscle innervated by the caudal segment (the 'contiguous pattern' in online supplementary figure S1). On the other hand, if the abnormalities are observed only in the muscle innervated by the caudal segment while the muscle of the rostral segment remains intact (the 'non-contiguous (skipping) pattern' in online supplementary figure S1), the results cannot be attributed to differences in motoneuronal vulnerability. We also examined the first dorsal interosseous (FDI; mainly innervating segment: C8), L3 paraspinalis (L3PS), rectus femoris (RF; L3/4), tibialis anterior (TA; L4/5, mainly L5) and medial head of the gastrocnemius (GC; S1/2, mainly S1).[23–26]

### Needle electromyography

Spontaneous EMG activities were detected with a conventional concentric needle electrode (recording surface area: 0.3 $mm^2$) in the above-mentioned muscles on the ipsilateral side of symptom onset in the upper limb onset patients and on the right side in the patients with bulbar or respiratory onset. For evaluation of paraspinal muscles, we examined the multifidus muscles, which are innervated by a single segment.[28]

Fibrillation potentials and positive sharp waves (Fib/PSWs) were explored at 10 different sites in each muscle. Fib/PSWs were diagnosed to be pathological only when they were identified at more than two different sites within the muscle. The fasciculation potential (FP) was defined as a potential that was similar in shape to the motor unit potential (MUP) and fired in a highly irregular pattern, often with a clustering of discharges. We identified FPs only when potentials of the same shape appeared at least twice. To detect FPs, we observed spontaneous activity at one site in each muscle for 60–90 s, which is sufficiently long enough to confirm the reproducibility of FPs.[29] Any persistence of voluntary MUPs was considered to render the identification of FPs impossible. We considered the examined muscles to be involved if Fib/PSWs, FPs or both were observed. Considering their higher objectivity beyond multicentre and burdens of patients, only spontaneous activities were adopted to prove LMN involvements in this study.

All EMG examinations were performed by proficient electromyographers with at least 5 years of professional EMG experience (TS, TK, KS and YN).

### Data analysis

Frequencies of the presence of abnormal spontaneous EMG activity were compared among the examined muscles by performing multiple comparisons with Fisher's exact probability test and the p value adjustment method of Holm. p Values less than 0.05 were considered to be significant.

### Standard protocol approvals, registrations and patient consents

The local ethics committees of Tokyo Medical and Dental University School of Medicine, Chiba University Graduate School of Medicine, Kyoto Prefectural University of Medicine, Musashino Red Cross Hospital, Kanto Central Hospital and Nakano General Hospital approved this study. All patients gave us informed consents for the procedures.

## RESULTS

Of the 40 patients with sporadic ALS included in this study, we ultimately analysed data from 36 patients (23 men, 13 women) because sufficient data for the paired paraspinal and thigh muscles were not obtained in 4 patients. The ages of 36 patients ranged from 41 years to 79 years (mean 63.3). The diagnoses were definite ALS in 8 patients, probable in 14 and probable-laboratory-supported in 14 according to the revised El Escorial criteria. Symptom onset occurred in the bulbar region in 10 patients, in the upper limb in 25 patients and as respiratory symptoms in 1 patient. The mean duration from symptom onset to the nEMG study was 16.9 months (range 3–84).

The full nEMG data for the 36 patients are shown in figure 1, online supplementary figure S2A,B. Abnormal spontaneous EMG activity was present in the FDI of all 36 patients. The distribution patterns of nEMG abnormalities among the spinal segments could be divided into three types: diffuse, contiguous and non-contiguous (skipping) patterns. The diffuse pattern was observed in 19 patients (53%); of these, 13 (patients 1–13) showed abnormal nEMG findings at all examined muscles and 6 (patients 14–19) showed abnormalities at every examined spinal segment, although not at all muscles. The contiguous pattern was found in three patients (8.3%; patients 20–22) in whom abnormal findings were detected in all examined segments except S1—the most remote segment from the onset site. One

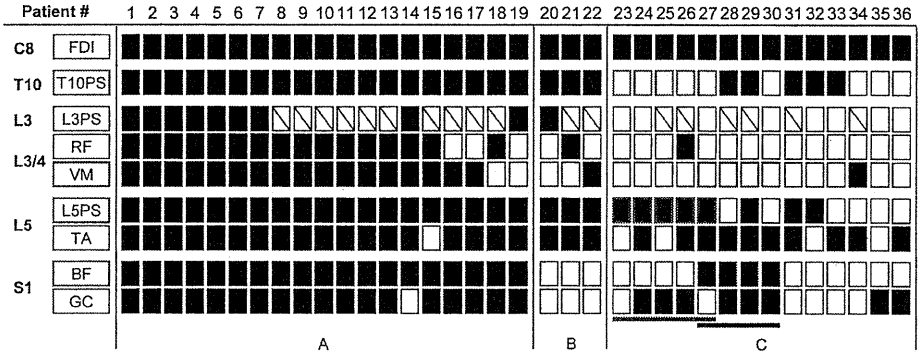


**Figure 1** Distribution patterns of needle electromyography (nEMG) abnormality in all patients. Closed squares: abnormal spontaneous EMG activity present. Open squares: abnormal spontaneous EMG activity absent. Squares with oblique line: data not available. (A) Diffuse pattern. (B) Contiguous pattern. (C) Non-contiguous (skipping) pattern. Note that the rostrally absent and caudally present spontaneous activity pattern between paired muscles with the same motoneuronal vulnerability is evident in the paraspinal muscle pair (green, patients 23–27) and the thigh muscle pair (red, patients 27–30) in 8 of 14 patients with the skipping pattern. The non-contiguous (skipping) pattern was present in both muscle pairs in patient 27.

of these three patients (patient 22) also showed the contiguous pattern in the thigh muscle pair; that is, an abnormality was evident in VM but not in BF. The non-contiguous (skipping) pattern was found in 14 patients (39%; patients 23–36), in whom abnormal spontaneous activities were detected from C8 to more caudal segments with skipping of intermediate segments such as T10 or L3/4. Representative nEMG findings of the non-contiguous pattern in a patient with bulbar onset (patient 27) are shown in figure 2.

Eight of the 14 patients also exhibited the non-contiguous pattern in the paired muscles; of these, five (patients 23–27) showed the pattern in the paraspinal muscle pair (involvement of L5PS with skipping of T10PS) (table 1A), four (patients 27–30) showed the pattern in the thigh muscle pair (involvement of BF innervated by S1 with skipping of VM innervated by L3/4) (table 1B). One of the eight patients (patient 27) showed this pattern in both pairs.

In order to consider whether there is a local propagation of the non-contiguously affected lumbosacral lesion, we used schematics to examine the anatomical distributions of the involved motoneuron pools of the lumbosacral muscles in the eight patients who exhibited the skipping pattern in the paired muscles (figure 3).[23–26 30 31] The involved motoneuron pools were located in close horizontal or radial proximity to one another in five patients (patients 26–30) and appeared to form a cluster in four patients (patients 27–30). By contrast, the involved motoneuron pools were not horizontally contiguous in two patients (patients 24–25). The one remaining patient (patient 23) had only one lesion in the lumbosacral muscles.

Excluding FDI, which was involved in all patients, the percentage of patients with nEMG abnormalities was the highest in TA (13/17, 76.5%) and L5PS (11/17, 64.7%) and was the lowest in RF and VM (2/17, 11.8%) (figure 4). Pairwise comparisons among the muscles showed statistically significant differences in proportions between the muscles innervated by L3/4 and L5: RF and TA (p=0.01), RF and L5PS (p=0.03), VM and TA (p=0.01), and VM and L5PS (p=0.03). There were no

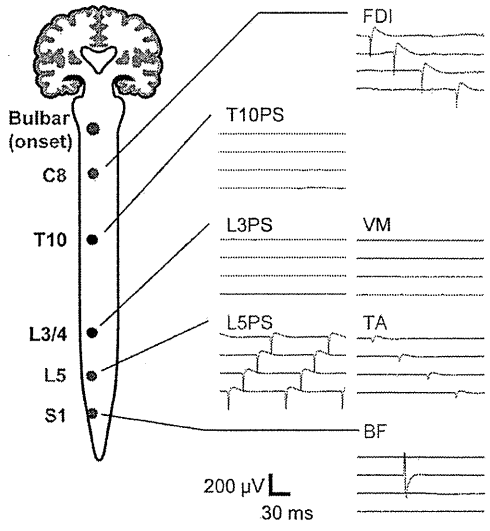


**Figure 2** Representative needle electromyography (nEMG) finding in the patient with non-contiguous pattern. nEMG finding of patient 27 whose onset was bulbar symptoms. Positive sharp waves (first dorsal interosseous (FDI), L5PS and tibialis anterior (TA)) or a fasciculation potential (biceps femoris (BF)) are present with skipping of the muscles innervated by intermediate segments. Note that the non-contiguous (skipping) distribution pattern is evident between the muscles of the paraspinal (T10PS and L5PS) and thigh (vastus medialis (VM) and BF) pairs. Red type indicates nEMG abnormalities.

**Table 1** Frequencies of nEMG abnormality patterns in paired muscles among 14 patients with a non-contiguous (skipping) pattern

| | | | | |
|---|---|---|---|---|
| (A) The patterns in the paraspinal muscle pairs | | | | |
| FDI (C8) | + | + | + | + |
| T10PS | – | + | + | – |
| L5PS | – | – | + | + |
| Number of patients | 4 | 2 | 3 | 5 |
| (B) The patterns in the thigh muscle pairs | | | | |
| FDI (C8) | + | + | + | + |
| VM (L3/4) | – | + | + | – |
| BF (S1) | – | – | + | + |
| Number of patients | 9 | 1 | 0 | 4 |

+, abnormal spontaneous EMG activities present; –, abnormal spontaneous activities absent; BF, biceps femoris; FDI, first dorsal interosseous; T10PS, T10 paraspinalis; L5PS, L5 paraspinalis; VM, vastus medialis.

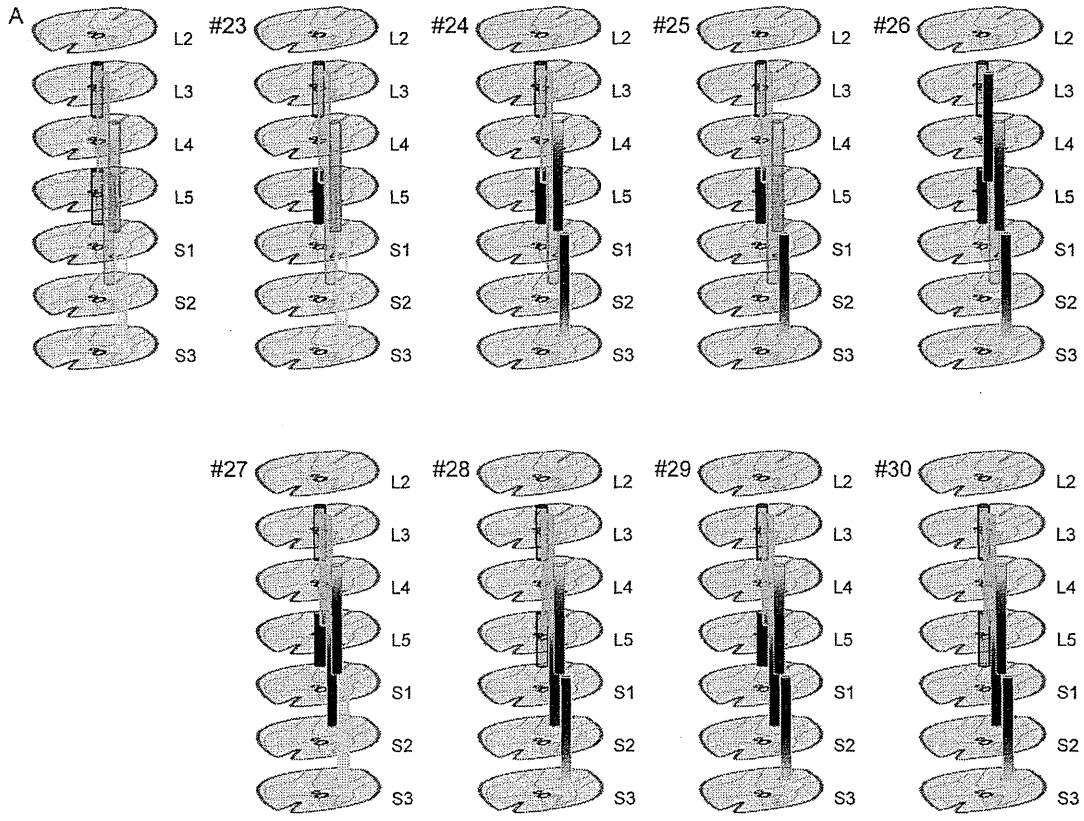


**Figure 3** Schematic diagrams of motoneuron pools of the examined muscles in the lumbosacral cord (A) and their patterns of involvement in eight patients showing the non-contiguous (skipping) pattern in the paired muscles (patients 23–30). The locations of motoneuron pools innervating each muscle were taken from refs [23–26 30] and [31]. Note that the involved motoneuron pools (darkly shaded) appear to neighbour one another in 3-dimensional anatomy, and appear to form a cluster for four patients (patients 27–30) in particular. VM (orange column), vastus medialis deep layer; RF (orange column), rectus femoris; L3 PS (upper red column), paraspinal muscle at L3 level; TA (pink column), tibialis anterior; L5 PS (lower red column), paraspinal muscle at L5 level; BF (green column), biceps femoris long head; GC (yellow column), gastrocnemius medial head.

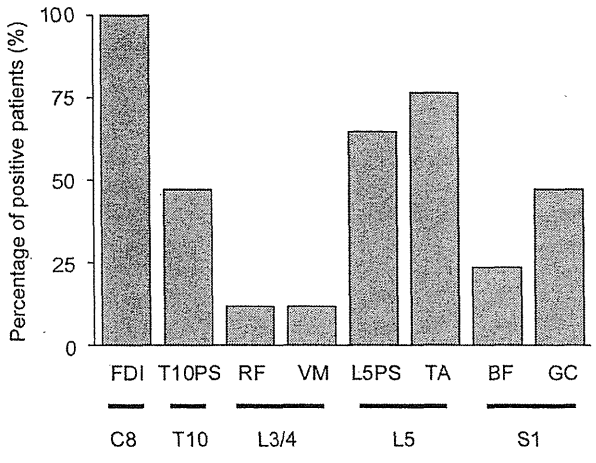


**Figure 4** Frequency of needle electromyography abnormality of each muscle in the patients with contiguous and non-contiguous distribution patterns. With the exception of first dorsal interosseous (FDI) which, as the most rostral muscle, was affected in all patients, the highest frequencies were found in the muscles innervated by L5 and the lowest in the muscles innervated by L3/4. The differences were statistically significant ($p<0.05$, Fisher's exact probability test using the p value adjustment method of Holm). Note that the frequencies are almost same between L5PS and tibialis anterior (TA).

statistically significant differences in other pairs of muscles except those including FDI.

We also investigated and compared the frequency of Fib/PSWs and that of FPs in every muscle of all included patients (figure 5). Fib/PSWs were more frequently observed than FPs in FDI (C8), which was the onset region in most of the included patients. To the contrary, FPs were dominantly observed than Fib/PSWs in RF or VM (L3/4) and BF or GC (S1), away from the onset region. However, TA and L5PS, both of which are innervated by L5, showed Fib/PSWs less rarely than FPs.

## DISCUSSION

We investigated whether the involvement of LMNs in sporadic ALS spreads contiguously in the rostrocaudal direction from the onset site. If prion-like propagation underlies the progression of ALS and the disease pathology in the first focal lesion propagates to adjacent cells in a cell-to-cell domino-like manner (the 'single seed and simple propagation' hypothesis) (see online supplementary figure S3A), involved LMNs should be distributed contiguously from the onset site.

Our nEMG study revealed that more than 50% of patients showed diffuse patterns. They showed weakness or muscle atrophy in lumbosacral regions more frequently than the rest (79% vs 29%). Therefore, they seemed to be in later stages of the disease.

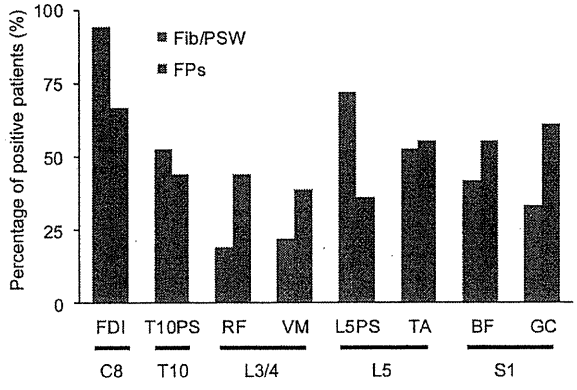


**Figure 5** The comparison of frequencies between fibrillation potentials, positive sharp waves (Fib/PSWs) and fasciculation potentials (FPs) of each muscle in all patients. Blue bar: Fib/PSWs, Red bar: FPs. FPs, known to precede Fib/PSWs, were shown more frequently than Fib/PSWs in the all lumbosacral segments but L5, suggesting that L5 segment was involved earlier than other lumbosacral segments.

In 14 of 17 patients, after excluding patients with the diffuse pattern, the abnormalities were distributed non-contiguously from the onset site, with skipping of intermediate spinal segments. The non-contiguous distribution of nEMG abnormalities may merely represent false-negative nEMG results in the 'skipped' segments where LMNs have in fact been involved. Two kinds of false negatives are conceivable: that based on methodological limitations, and that due to the time lag from molecular disease onset. First, given that a needle electrode has a limited pick-up area, evaluating all motor units (MU) in a muscle is practically impossible. Second, a time lag must exist because many molecular changes occur before they reach a threshold at which spontaneous EMG activities can be detected. Individual LMNs have different vulnerabilities in ALS;[9 19–21] more vulnerable LMNs will degenerate faster than more resistant ones even if the pathological molecular process begins simultaneously. Therefore, the failure to detect abnormal EMG activities in skipped spinal segments may simply have been caused by the lower vulnerability of neurons at these sites, if less vulnerable LMNs are radially sandwiched by the highly vulnerable LMNs of more rostral and caudal segments.

However, we consider it unlikely that they alone could produce the non-contiguous pattern. The sensitivities for detecting spontaneous EMG activity should be very similar in the two thigh muscles (VM and BF) and in the paraspinal muscles (T10 and L5) we examined. First, this is because the total number of insertions was fixed in every muscle by the same examiner. Second, the motoneuronal vulnerabilities as well as the sensitivities are expected to be nearly identical between the paired muscles because the lengths of their innervating motor axons are very similar and they have similar proportions of type I/II muscle fibres. Taken together, the probability of false negatives should be nearly same between the paired muscles. Therefore, the segmental distribution of ALS lesions can be non-contiguous along the spinal cord in the early stage of the disease (see online supplementary figure S3B).

Krarup claimed that abnormal spontaneous activities in nEMG are not as sensitive as changes in MUPs.[32] We have searched these chronic neurogenic changes in VM/RF of the four patients who showed non-contiguous pattern in thigh pair of muscles. Although one patient (patient 28) showed polyphasic MUPs in RF, the other three patients are still classified as non-contiguous pattern with evaluating chronic changes, and therefore, our conclusion remains unchanged. In fact, which kind of neurogenic changes appears the earliest in nEMG of ALS patients still remains controversial. Recently, de Carvalho *et al*[33] have reported that FPs are the earliest changes in ALS patients.

Both the spreading mechanisms of toxic factors, namely, simple diffusion of soluble toxic factors and cell-to-cell propagation from the only onset site are inconsistent with these non-contiguous distributions. The former mechanism should show abnormalities in anatomically proximal segments to onsets such as T10/L3 earlier than L5/S1. Assuming the latter mechanism, it is important to note that the lateral motor columns of the anterior horn innervating distal limb muscles are not structurally contiguous between the cervical and lumbosacral spinal cords.[30] By contrast, the medial motor column, which innervates axial muscles, extends contiguously from the lower medulla to the lumbar spinal cord. This indicates that regional spread from FDI to TA needs to have three steps; (1) disease transfer from lateral to medial motor column in cervical segment, (2) caudal propagation along the medial column and (3) disease transfer from medial to lateral motor column in lumbosacral segments. If ALS lesions spread along the medial column in the rostrocaudal direction by cell-to-cell propagation, our results showing the skipping of T10PS or L3PS in 11 of the 14 patients with non-contiguous pattern cannot be explained. Taken together, whatever mechanisms can underlie the consequent spread, we conclude that ALS progression is not explained by single onset site, but by multiple onset sites. This speculation is consistent with the fact that there are ALS patients who have onsets in two regions simultaneously.[14]

Rostral lesions were found to spread significantly more frequently to the TA and L5PS than L3/4 innervating muscles. Other investigators also demonstrated that abnormal spontaneous EMG activities were detected more frequently at the TA than at the quadriceps in ALS.[34 35] It is noteworthy that the L5PS was also highly involved in our study. Some electromyographers claim that the paraspinalis at the lower lumbar spine may show Fib/PSWs even in healthy subjects.[36] However, Fib/PSWs were not detected in normal subjects who did not have any abnormality of the lumbar spine on MRI,[37] and we also selected ALS patients without lumbar spine abnormalities on MRI. The fact that the involvement was almost identical between the TA and L5PS was unexpected, although a previous report showed a similar result in the early stage of ALS,[38] because LMNs of L5PS are generally considered less vulnerable than those of TA in ALS; LMNs innervating paraspinal muscles have shorter axons and smaller cell bodies than LMNs innervating distal muscles. These considerations imply a horizontal spread of ALS pathology from the more vulnerable neurons innervating the TA to the less vulnerable neurons innervating the L5PS within the L5 segment.

Another possible explanation for the frequent involvement of LMNs in the TA and L5PS is that L5 itself as a segment might be more vulnerable to ALS than other lumbosacral segments. ALS patients have lumbar spondylosis more frequently than the general population at corresponding ages,[39 40] although lumbar spondylosis was carefully excluded in our study by detailed MRI examinations. The L5 segment accounted for 90.3% of 112 vertebrae in Japanese patients with lumbar spondylosis.[40] Daily repetitive movements of the lumbar spine may cause weight-bearing biomechanical stresses particularly on L5, possibly inducing chronic minor trauma of the nerve root. Experimentally,

injuries to the anterior root have been demonstrated to produce mislocalisation of TDP-43 in spinal motoneurons.[41] These considerations suggest an L5 segmental vulnerability to ALS lesions, but among cervical segments, the segment C8 innervating FDI which is the most vulnerable in ALS,[7 9 10 34] is different from the segment that is commonly affected in cervical spondylosis.[42]

Kiernan and his colleagues have reported that cortical hyperexcitability is an early feature in ALS, and UMN and LMN dysfunction coexists.[43] We cannot take account of the influence of UMN impairments by spontaneous EMG activities we have investigated, hence we reviewed the clinical UMN features of the 14 patients who showed 'non-contiguous pattern' at nEMG examination (see online supplementary table S1). We can assume that they should show UMN features in both onset and lumbosacral regions if the non-contiguous pattern of nEMG is driven by the preceding UMN involvements. However, our results showed no UMN features were revealed in cervical regions in five patients (patients 23, 24, 30, 32, 35) and in lumbosacral regions in three patients (patients 24, 30, 33), neither. This result indicates the existence of some skipping mechanisms of LMN involvements regardless of UMN in propagation of ALS. On the other hand, UMN features were widespread in the rest of the patients of non-contiguous pattern. Especially, hyperreflexia was simultaneously shown in both patella tendon (quadriceps femoris; L3/4) and Achilles tendon (GC and soleus; S1) to almost the same degree even in the patients with L3/4 skipping pattern. From these findings, we could not indicate that cortical hyperexcitability is driving the non-contiguous spread of LMN involvement in ALS. However, it is well documented that cortical hyperexcitability evaluated by short intracortical inhibition with threshold tracking transcranial magnetic stimulation techniques precedes clinical UMN features,[43] which is supported by the neuropathological examination that 50% of progressive muscular atrophy patients had pyramidal tract degeneration.[44] Therefore, more detailed electrophysiological analysis is needed for elucidating the role of upper motor neuron dysfunction on this non-contiguous spread, because it is a potential target of therapeutic intervention, especially riluzole.[45 46]

FPs are considered to appear in the muscles which are in the earlier stage of involvement and are involved more slightly, especially the muscles which is located away from onset region, while Fib/PSWs tend to appear later than FPs and tend to appear in the onset muscle.[32 33 47] The fact that only L5 innervating muscles in the lumbosacral regions show Fib/PSWs less rarely than FPs suggests that L5 segment is involved at first in the lumbosacral regions and then neighbouring segments are subsequently involved.

We also analysed the anatomical distribution of the involved motoneuron pools of the lumbosacral segments in the eight patients with non-contiguously affected lumbosacral lesions. The involved motoneuron pools were located in close proximity to one another horizontally or radially, appearing to form a cluster in four patients. Local propagation of pathology between motor columns can exist after the second hit in the lumbosacral cord following the first hit at the rostral onset site (see online supplementary figure S3B). If it is true, for explanation for horizontal spread between distinct motor columns, we have to assume a different mechanism from neuron-to-neuron protein transfer; for example, diffusion of a secreted toxic soluble factor or glia-to-neuron interaction which is known in the mutant SOD1 transgenic mouse[48] may play a role in a transmission between motor columns.

In conclusion, the results of our prospective study and detailed nEMG results in 36 ALS patients showed that LMN involvement in many early stage ALS patients was distributed non-contiguously in the rostrocaudal direction of the spinal segments, indicating that the onset site is not single even with consideration of difference in motoneuronal vulnerability. On the other hand, local involvements of the anterior horn lesions tended to be formed as some clusters, and therefore, we here propose 'multifocal hits and local propagation' as a new hypothesis for one of the mechanisms of ALS progression.

**Author affiliations**
[1]Department of Neurology and Neurological Science, Graduate School, Tokyo Medical and Dental University, Tokyo, Japan
[2]Clinical Laboratory, Tokyo Medical and Dental University Hospital of Medicine, Tokyo, Japan
[3]Department of Neurology, Graduate School of Medicine, Chiba University, Chiba, Japan
[4]Department of Neurology, Graduate School of Medical Science, Kyoto Prefectural University of Medicine, Kyoto, Japan
[5]Department of Neurology, Musashino Red Cross Hospital, Tokyo, Japan
[6]Department of Neurology, Kanto Central Hospital, Tokyo, Japan
[7]Department of Neurology, Nakano General Hospital, Tokyo, Japan

**Acknowledgements** We sincerely thank Dr Nobuo Sanjo, Hiroyuki Tomimitsu, Takuya Ohkubo, Taro Ishiguro, Akira Machida, Makoto Takahashi, Yuji Hashimoto and Masahiko Ichijo (Department of Neurology and Neurological Science, Graduate School, Tokyo Medical and Dental University); Dr Shuta Toru (Department of Neurology, Nakano General Hospital); Dr Hiroaki Yokote (Department of Neurology, Musashino Red Cross Hospital); Dr Zen Kobayashi and Yoshiyuki Numasawa (Department of Neurology, JA Toride Medical Center); Dr Masato Obayashi (Department of Neurology, National Disaster Medical Center); Dr Minoru Kotera and Yoko Ito (Department of Neurology, Tsuchiura Kyodo Hospital); Dr Kotaro Yoshioka (Department of Neurology, Yokohama City Minato Red Cross Hospital); Dr Mutsufusa Watanabe and Dr Hiroya Kuwahara (Department of Neurology, Tokyo Metropolitan Bokutoh Hospital); Dr Osamu Tao (Department of Neurology, Ome Municipal General Hospital); and Dr Kazuaki Kanai (Department of Neurology, Graduate School of Medicine, Chiba University) for their excellent technical assistance and referral of patients.

**Contributors** TS, TK, KS, SM, SK and TY designed the study. TS, TK, KS, Y-iN, YY, AI and KA conducted the examinations. TS and TK performed statistical analysis. TS, TK and TY drafted the manuscript. SO, TK, TK, MN, HM and TY supervised the study. The version to be published was approved by all of the authors. TS accepts full responsibility for the data as the guarantor.

**Funding** This research was supported by a Grant-in-Aid for Scientific Research (A) to Yokota (#22240039); a Grant-in-Aid for Exploratory Research to Kanouchi. (#24659425); and Research on Neurodegenerative Diseases/ALS from the Ministry of Health, Labour, Welfare, Japan to Mizusawa; and Strategic Research Program for Brain Science, Field E from Ministry of Education, Culture, Sports and Technology, Japan to Mizusawa.

**Competing interests** None.

**Patient consent** Obtained.

**Ethics approval** The local ethics committees of Tokyo Medical and Dental University School of Medicine (No. 1091), Chiba University Graduate School of Medicine (No. 769), Kyoto Prefectural University of Medicine (No. E-367), Musashino Red Cross Hospital (No. 26), Kanto Central Hospital (No. 1 of Jan 12, 2012) and Nakano General Hospital (No. 23-005) approved this study.

**Provenance and peer review** Not commissioned; externally peer reviewed.

**Data sharing statement** The principal investigator: Teruhiko Sekiguchi has full access to all of the patients' clinical data including EMG results and takes full responsibility for the data, the accuracies of analyses and interpretation, and the conduct of the research.

## REFERENCES

1 Goedert M, Clavaguera F, Tolnay M. The propagation of prion-like protein inclusions in neurodegenerative diseases. *Trends Neurosci* 2010;33:317–25.
2 Polymenidou M, Cleveland DW. The seeds of neurodegeneration: prion-like spreading in ALS. *Cell* 2011;147:498–508.
3 Grad LI, Guest WC, Yanai A, *et al*. Intermolecular transmission of superoxide dismutase 1 misfolding in living cells. *Proc Natl Acad Sci USA* 2011;108:16398–403.
4 Furukawa Y, Kaneko K, Watanabe S, *et al*. A seeding reaction recapitulates intracellular formation of Sarkosyl-insoluble transactivation response element (TAR) DNA-binding protein-43 inclusions. *J Biol Chem* 2011;286:18664–72.

5 DeJesus-Hernandez M, Mackenzie IR, Boeve BF, *et al*. Expanded GGGGCC hexanucleotide repeat in noncoding region of C9ORF72 causes chromosome 9p-linked FTD and ALS. *Neuron* 2012;72:245–56.
6 Munch C, O'Brien J, Bertolotti A. Prion-like propagation of mutant superoxide dismutase-1 misfolding in neuronal cells. *Proc Natl Acad Sci USA* 2011;108:3548–53.
7 Swash M. Vulnerability of lower brachial myotomes in motor neurone disease: a clinical and single fibre EMG study. *J Neurol Sci* 1980;47:59–68.
8 Swash M, Leader M, Brown A, *et al*. Focal loss of anterior horn cells in the cervical cord in motor neuron disease. *Brain* 1986;109:939–52.
9 Tsukagoshi H, Yanagisawa N, Oguchi K, *et al*. Morphometric quantification of the cervical limb motor cells in controls and in amyotrophic lateral sclerosis. *J Neurol Sci* 1979;41:287–97.
10 Kanouchi T, Ohkubo T, Yokota T. Can regional spreading of ALS motor symptoms be explained by prion-like propagation? *J Neurol Neurosurg Psychiatry* 2012;83:739–45.
11 Ravits J, Paul P, Jorg C. Focality of upper and lower motor neuron degeneration at the clinical onset of ALS. *Neurology* 2007;68:1571–5.
12 Ravits J, La Spada AR. ALS motor phenotype heterogeneity, focality, and spread: deconstructing motor neuron degeneration. *Neurology* 2009;73:805–11.
13 Körner S, Kollewe K, Fahlbusch M, *et al*. Onset and spreading patterns of upper and lower motor neuron symptoms in amyotrophic lateral sclerosis. *Muscle Nerve* 2011;43:636–42.
14 Fujimura-Kiyono C, Kimura F, Ishida S, *et al*. Onset and spreading patterns of lower motor neuron involvements predict survival in sporadic amyotrophic lateral sclerosis. *J Neurol Neurosurg Psychiatry* 2011;82:1244–9.
15 Rabin SJ, Kim JM, Baughn M, *et al*. Sporadic ALS has compartment-specific aberrant exon splicing and altered cell-matrix adhesion biology. *Hum Mol Genet* 2010;19:313–28.
16 Gargiulo-Monachelli GM, Janota F, Bettini M, *et al*. Regional spread pattern predicts survival in patients with sporadic amyotrophic lateral sclerosis. *Eur J Neurol* 2012;19:834–41.
17 Wohlfart G. Collateral regeneration in partially denervated muscles. *Neurology* 1958;8:175–80.
18 Brooks BR, Miller RG, Swash M, *et al*. El Escorial revisited: revised criteria for the diagnosis of amyotrophic lateral sclerosis. *Amyotroph Lateral Scler Other Motor Neuron Disord* 2000;1:293–9.
19 Haverkamp LJ, Appel V, Appel SH. Natural history of amyotrophic lateral sclerosis in a database population. Validation of a scoring system and a model for survival prediction. Brain 1995;118:707–19.
20 Cappellari A, Brioschi A, Barbieri S, *et al*. A tentative interpretation of electromyographic regional differences in bulbar- and limb-onset ALS. *Neurol* 1999;52:644–6.
21 Pun S, Santos AF, Saxena S, *et al*. Selective vulnerability and pruning of phasic motoneuron axons in motoneuron disease alleviated by CNTF. *Nat Neurosci* 2006;9:408–19.
22 Mannion AF, Weber BR, Dvorak J, *et al*. Fibre type characteristics of the lumbar paraspinal muscles in normal healthy subjects and in patients with low back pain. *J Orthop Res* 1997;15:881–7.
23 Liguori R, Krarup C, Trojaborg W. Determination of the segmental sensory and motor innervation of the lumbosacral spinal nerves: an electrophysiological study. *Brain* 1992;115:915–34.
24 Perotto AO. *Anatomical guide for the electromyographer: the limbs and trunk*, 5th edn. Springfield, IL: Charles C Thomas, 2011:21–250.
25 Wilbourn AJ, Aminoff MJ. AAEE minimonograph #32: the electrophysiologic examination in patients with radiculopathies. *Muscle Nerve* 1998;11:1099–114.
26 Tsao BE, Levin KH, Bodner RA. Comparison of surgical and electrodiagnostic findings in single root lumbosacral radiculopathies. *Muscle Nerve* 2003;27:60–4.
27 Johnson MA, Polgar J, Weightman D, *et al*. Data on the distribution of fibre types in thirty-six human muscles. An autopsy study. *J Neurol Sci* 1973;18:111–29.
28 Haig AJ, Moffroid M, Henry S, *et al*. A technique for needle localization in paraspinal muscles with cadaveric confirmation. *Muscle Nerve* 1991;14:521–6.
29 Mills KR. Detecting fasciculations in amyotrophic lateral sclerosis: duration of observation required. *J Neurol Neurosurg Psychiatry* 2011;82:549–51.
30 Routal RV, Pal GP. A study of motoneuron groups and motor columns of the human spinal cord. *J Anat* 1999;195:211–24.
31 Carpenter MB. *Human neuroanatomy*, 8th edn. Baltimore: Williams & Wilkins, 1983:252–4.
32 Krarup C. Lower motor neuron involvement examined by quantitative electromyography in amyotrophic lateral sclerosis. *Clin Neurophysiol* 2011;122:414–22.
33 de Carvalho M, Swash M. Fasciculation potentials and earliest changes in motor unit physiology in ALS. *J Neurol Neurosurg Psychiatry* 2013;84:963–8.
34 Kuncl RW, Cornblath DR, Griffin JW. Assessment of thoracic paraspinal muscles in the diagnosis of ALS. *Muscle Nerve* 1988;11:484–92.
35 Noto Y, Misawa S, Kanai K, *et al*. Awaji ALS criteria increase the diagnostic sensitivity in patients with bulbar onset. *Clin Neurophysiol* 2012;123:382–5.
36 Date ES, Mar EY, Bugola MR, *et al*. The prevalence of lumbar paraspinal spontaneous activity in asymptomatic subjects. *Muscle Nerve* 1996;19:350–4.
37 Haig AJ, Tong HC, Yamakawa KS, *et al*. The sensitivity and specificity of electrodiagnostic testing for the clinical syndrome of lumbar spinal stenosis. *Spine* 2005;30:2667–76.
38 de Carvalho MA, Pinto S, Swash M. Paraspinal and limb motor neuron involvement within homologous spinal segments in ALS. *Clin Neurophysiol* 2008;119:1607–13.
39 Yamada M, Furukawa Y, Hirohata M. Amyotrophic lateral sclerosis: frequent complications by cervical spondylosis. *J Orthop Sci* 2003;8:878–81.
40 Sakai T, Sairyo K, Takao S, *et al*. Incidence of lumbar spondylolysis in the general population in Japan based on multidetector computed tomography scans from two thousand subjects. *Spine* 2009;34:2346–50.
41 Moisse K, Volkening K, Leystra-Lantz C, *et al*. Divergent patterns of cytosolic TDP-43 and neuronal progranulin expression following axotomy: implications for TDP-43 in the physiological response to neuronal injury. *Brain Res* 2009;1249:202–11.
42 Yoss RE, Corbin KB, Maccarty CS, *et al*. Significance of symptoms and signs in localization of involved root in cervical disk protrusion. *Neurology* 1957; 7:673–83.
43 Vucic S, Kiernan MC. Novel threshold tracking techniques suggest that cortical hyperexcitability is an early feature of motor neuron disease. *Brain* 2006;129:2436–46.
44 Kim WK, Liu X, Sandner J, *et al*. Study of 962 patients indicates progressive muscular atrophy is a form of ALS. *Neurology* 2009;73:1686–92.
45 Vucic S, Lin CS, Cheah BC, *et al*. Riluzole exerts central and peripheral modulating effects in amyotrophic lateral sclerosis. *Brain* 2013;136:1361–70.
46 Stefan K, Kunesch E, Benecke R, *et al*. Effects of riluzole on cortical excitability in patients with amyotrophic lateral sclerosis. *Ann Neurol* 2001;49:536–9.
47 Okita T, Nodera H, Shibuta Y, *et al*. Can Awaji ALS criteria provide earlier diagnosis than the revised El Escorial criteria? *J Neurol Sci* 2011;302:29–32.
48 Boillée S, Yamanaka K, Lobsiger CS, *et al*. Onset and progression in inherited ALS determined by motor neurons and microglia. *Science* 2006;312:1389–92.

# Spreading of amyotrophic lateral sclerosis lesions—multifocal hits and local propagation?

Teruhiko Sekiguchi, Tadashi Kanouchi, Kazumoto Shibuya, et al.

*J Neurol Neurosurg Psychiatry* 2014 85: 85-91 originally published online September 11, 2013
doi: 10.1136/jnnp-2013-305617

Gait & Posture 37 (2013) 264–268

Contents lists available at SciVerse ScienceDirect

Gait & Posture

journal homepage: www.elsevier.com/locate/gaitpost

# Posterior tibial tendon dysfunction and flatfoot: Analysis with simulated walking

Kota Watanabe [a,b], Harold B. Kitaoka [a], Tadashi Fujii [a], Xavier Crevoisier [a], Lawrence J. Berglund [a], Kristin D. Zhao [a], Kenton R. Kaufman [a], Kai-Nan An [a,*]

[a] Department of Orthopedic Surgery, Mayo Clinic, Rochester, MN, USA
[b] Department of Orthopedic Surgery, Sapporo Medical University School of Medicine, Sapporo, Japan

ARTICLE INFO

*Article history:*
Received 11 October 2011
Received in revised form 16 July 2012
Accepted 21 July 2012

*Keywords:*
Flatfoot
Kinematics
Simulator
Cadaver
Gait simulation

ABSTRACT

Many biomechanical studies investigated pathology of flatfoot and effects of operations on flatfoot. The majority of cadaveric studies are limited to the quasistatic response to static joint loads. This study examined the unconstrained joint motion of the foot and ankle during stance phase utilizing a dynamic foot–ankle simulator in simulated stage 2 posterior tibial tendon dysfunction (PTTD). Muscle forces were applied on the extrinsic tendons of the foot using six servo-pneumatic cylinders to simulate their action. Vertical and fore-aft shear forces were applied and tibial advancement was performed with the servomotors. Three-dimensional movements of multiple bones of the foot were monitored with a magnetic tracking system. Twenty-two fresh-frozen lower extremities were studied in the intact condition, then following sectioning peritalar constraints to create a flatfoot and unloading the posterior tibial muscle force. Kinematics in the intact condition were consistent with gait analysis data for normals. There were altered kinematics in the flatfoot condition, particularly in coronal and transverse planes. Calcaneal eversion relative to the tibia averaged 11.1 ± 2.8° compared to 5.8 ± 2.3° in the normal condition. Calcaneal-tibial external rotation was significantly increased in flatfeet from mean of 2.3 ± 1.7° to 8.1 ± 4.0°. There were also significant changes in metatarsal-tibial eversion and external rotation in the flatfoot condition. The simulated PTTD with flatfoot was consistent with previous data obtained in patients with PTTD. The use of a flatfoot model will enable more detailed study on the flatfoot condition and/or effect of surgical treatment.



## 1. Introduction

In recent years, there have been multiple reports related to posterior tibial tendon dysfunction (PTTD). PTTD is a common cause of acquired flatfoot deformity in adults; the condition may reach a prevalence of 10% in elderly women [1]. Most of the clinical investigations reported the effects of various operations to correct PTTD and flatfoot deformity, but *in vitro* and radiologic studies have also been published [2–5]. The optimum management of stage 2 PTTD [2] in which there is a mobile flatfoot has been a subject of debate for more than two decades. There are questions regarding the pathoanatomy of the deformity resulting from tendon dysfunction. A comprehensive understanding of the flatfoot malalignment will lead to more effective techniques for correcting it.

Previous investigators recognized the importance of defining the flatfoot and quantitating the degree of deformation [6]. Clinical measurements such as arch height have been used, but were not consistent between examiners [6]. Radiologic measurements of flatfoot have been performed in patients with PTTD [4,5]. Analysis of foot prints and ground reaction data in flatfeet have been reported [7]. Previous reports determined the contribution of various static elements in supporting the arch [8]. Others indicated that the posterior tibial tendon (PTT) plays a role in the dynamic support of the arch [3]. Most of these previous reports were *in vitro* studies with static loading of specimens. Recent gait analysis studies have revealed kinematics changes of the foot between normal and flatfoot [9–12]. *In vitro*, dynamic joint simulators have been developed recently for foot/ankle as well as other joints and applied for biomechanical studies of pathological situations of foot/ankle problems [13–19]. However, there have not been any publications, to our knowledge, detailing the three-dimensional kinematics of the flatfoot during simulated walking of the entire stance phase of gait.

We developed a dynamic foot–ankle simulator capable of recreating the stance phase of gait in cadaveric lower extremities [15]. It allows simulation of functional activities by allowing unconstrained motion of the foot and ankle while simultaneously applying time-histories of forces that affect the foot. A dynamic

* Corresponding author at: Mayo Clinic, 200 First Street SW, Rochester, MN 55905, USA. Tel.: +1 507 538 1717; fax: +1 507 284 5392.
*E-mail address:* an@mayo.edu (K.-N. An).

0966-6362/$ – see front matter © 2012 Elsevier B.V. All rights reserved.
http://dx.doi.org/10.1016/j.gaitpost.2012.07.015

simulator will be useful for improving our understanding of the mechanical behavior of the flatfoot compared to the normal foot. The purpose of the study was to examine unconstrained joint motion of the foot and ankle during stance phase in cadaveric lower extremities with simulated PTTD with flatfoot deformity utilizing a dynamic foot–ankle simulator.

## 2. Methods

Twenty-two fresh-frozen lower extremities were evaluated after gross visual screening for preexisting abnormalities of the foot. The mean age of the specimens was 78 years old (range, 47–95). Five were female, 17 male. Fourteen specimens were left feet and eight were right. The institutional research ethics committee reviewed and approved the study.

The custom simulator was able to subject cadaveric foot and ankle specimens to specified time-histories of normative ground reaction forces (GRF), and tendon loading based on physiological cross-sectional area (PCSA) and electromyography (EMG) data. Adjustments were made the initial muscle force profiles to match normal patterns of calcaneal-tibial angles and gross forefoot motion, while allowing totally unconstrained joint motions. The inputs were the forward tibial motion, fore-aft shear loading, tibial loading, and muscle loading. The outputs were measured foot reaction (force and center-of-pressure advancement) and joint kinematics. Since few biomechanical models were available for this hybrid (load and motion) control system, the tibial loading was prescribed to the normal vertical GRF profile as an approximation using a closed-loop servomotor so as to match the normal vertical GRF despite the disturbances from the muscle loading actuators. Ankle joint kinematics was controlled by muscle loading, which was initially targeted from the muscle gain, PCSA, and EMG data for each muscle group.

The leg specimen, amputated at the mid-tibial level, was potted in an acrylic plastic tube with polymethylmethacrylate cement, and fixed on the tendon loading unit (Fig. 1) [15]. The tendon-loading unit, consisting of six pneumatic cylinders, was connected through a linear ball screw to the servomotor tibial angle control unit, and through a hinge joint to the vertical loading unit. All the above units created a four-bar rocker configuration to control the angle of the loading unit or tibia relative to the ankle joint during the simulation. The vertical-loading unit, mounted on the frame, was connected to a linear slide powered by a linear ball screw and servomotor. This servomotor axis provided loading along the tibial axis by moving both the vertical loading unit and tendon loading unit onto the force plate. The sole of the foot contacted the custom-made force plate, which recorded the simulated vertical GRF. The bearing plate beneath the force plate allowed the relative forward translation of the foot and ankle and accommodated the anteroposterior shear force [20] by coupling the plate to another closed-loop servo axis. Most structures were built using non-metallic tubing or acrylic plastics, to minimize any interference with the magnetic tracking system.

The tibial angle control unit translated the tibial motion between 20° anterior and 40° posterior to vertical [21]. During testing, the tibial angle was monitored by a potentiometer. The tibial angle was used to determine the percentage of stance phase from the tibial angle history profile [21]. The estimated percent stance phase was used to prescribe the tendon and tibial loading [20,21]. The extrinsic muscles acting on or around the ankle were divided into six functional units: gastrocnemius-soleus, PTT, flexor hallucis longus-flexor digitorum longus, anterior tibial, extensor hallucis longus-extensor digitorum longus, and peroneus longus-peroneus brevis. A total of six pneumatic cylinders driven by servo-pneumatic valves were used to apply loads to the tendons. Sutures were attached to each tendon using a modified Krackow technique except for the Achilles tendon, which was sutured using a Leeds-Keio artificial ligament (Ellis Developments, Nottingham, UK) to sustain the comparable physiological loading. A uniaxial load cell was connected to each cylinder to monitor the load feedback signal to an IBM PC. A custom-written program (LabVIEW®, National Instruments, Austin, TX) was used for control and kinetic data acquisition. Tendon loads were estimated from PCSA and EMG data in the literature [20,22]. A linear EMG and force relationship was assumed [23,24]. An unknown muscle gain K and the corresponding cross sectional area (PCSAi) were multiplied by the relative EMG data (EMGi) to provide absolute forces to each cylinder ($Fi = K \times PCSAi \times EMGi$). To determine the unknown muscle gain or muscle stress, simulations were repeated until the gross foot–ankle kinematics matched reasonably well to the stance phase center-of-pressure and motion patterns, while the gain of the muscles was simultaneously adjusted. The applied vertical and fore-aft loads were reduced for the cadaver feet due to the limited suture strength and age of the specimens.

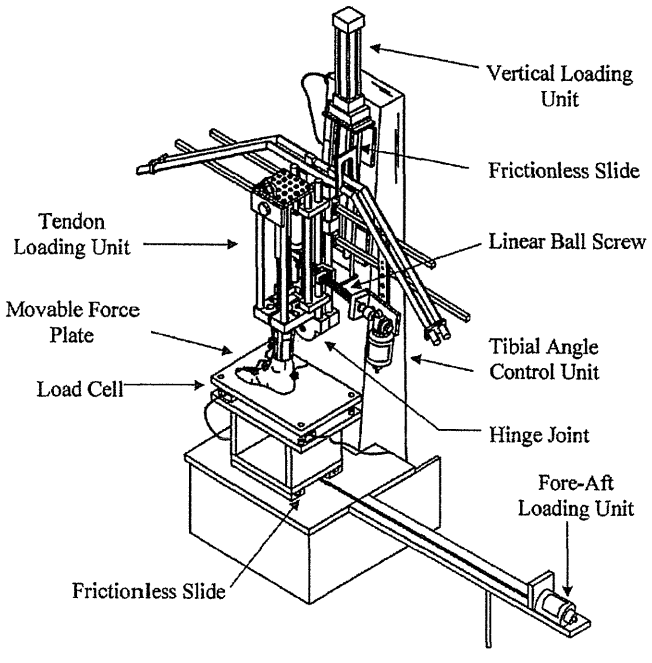


**Fig. 1.** Schematic drawing of the dynamic foot/ankle simulator.

Each specimen was cycled additional times through the entire stance phase to reduce the viscoelastic effect of soft tissues. The leg was then continuously moved from tibial flexion −20° (initial contact) to 40° flexion (pre-swing) while applying forces to the six muscle groups and subjecting it to the ground reaction force profiles. After testing the intact condition, a flatfoot condition was created by sectioning the peritalar soft tissue structures, including the spring ligament, long and short plantar ligaments, talocalcaneal interosseous ligament, medial talocalcaneal ligament, and tibionavicular portion of the superficial deltoid ligament. In order to simulate stage 2 PTTD and flatfoot, the posterior tibial muscle action was not simulated. A previous study [8] showed that flatfoot deformity occurred after these procedures, similar to that caused by stage 2 PTTD clinically. The applied vertical and fore-aft loads were not changed before and after the flatfoot model was created. Testing was performed three times for each condition and the average result was used for analysis.

Three-dimensional movements of the calcaneus and first metatarsus relative to the tibia were obtained with a magnetic tracking system (3Space Tracker System, Polhemus, Colchester, VT) [25,26]. The electromagnetic transmitter was fixed to the loading frame. Sensors were rigidly fixed to the anteromedial tibial diaphysis at the junction of the middle and distal thirds, posterolateral calcaneal body, and diaphysis of the dorsal-medial first metatarsal with acrylic mounting posts [26]. The relative angular motion between bones (calcaneal-tibial and first metatarsal-tibial) was expressed in terms of Eulerian angle description [25,26]. Bone positions were described relative to the previously described coordinate system [26]. The $x$-axis was oriented proximal-distal, the $y$-axis was oriented medial-lateral, and the $z$-axis was oriented anterior-posterior. The $x$-axis was along the tibial shaft through the ankle center, the $z$-axis was parallel to the projection of a line connecting the center of the heel and the second metatarsal on a plane perpendicular to the $x$-axis passing through the ankle center, and the $y$-axis was the product of the $x$- and $z$-axes following the right-hand rule passing through the ankle center. The three axes were also used to define the perpendicular planes: coronal ($x$–$y$ plane), sagittal ($x$–$z$ plane), and transverse ($y$–$z$ plane). Motion was defined as inversion and eversion in the coronal plane, dorsiflexion and plantarflexion in the sagittal plane, and internal rotation and external rotation in the transverse plane.

Statistical analysis was performed with a paired $t$-test, comparing the bony positions in the intact and flatfoot conditions. The level of significance was set at $p < 0.05$.

## 3. Results

All the results of angular motions of the calcaneus and the first metatarsal relative to the tibia are presented over an entire stance phase that started with heel strike and ended with toe-off (Fig. 2). Angular movement patterns were consistent across all specimens. In the sagittal plane, the forefoot contacted with the force plate at about 10% stance phase. Maximum dorsiflexion was observed at about 80% stance phase. Then rapid plantarflexion occurred until maximum plantarflexion at toe-off. In the coronal plane, the hindfoot (calcaneal-tibial) and forefoot (metatarsal-tibial) moved from an initial inversion at heel strike to eversion. Maximum eversion occurred at a late phase of stance, prior to heel rise. Then the foot progressively inverted until toe-off. In the transverse plane, the hindfoot and forefoot moved from an initial internal rotation to external rotation. At mid-stance the foot reversed and began to internal rotate until toe-off.